FINAL REPORT, CONTRACT NO. NAS8-20529

VOLUME 2

DEVELOPMENT OF A MICROMETEOROID SIMULATION DEVICE, CONSTANT AREA ACCELERATOR

7457/R1

SUBMITTED TO

GEORGE C. MARSHALL SPACE FLIGHT CENTER,
NATIONAL AERONAUTICS AND SPACE ADMINISTRATION,
HUNTSVILLE, ALABAMA, U.S.A.

24 OCTOBER 1967

COMPUTING DEVICES
OF CANADA LIMITED
AN AFFILIATE OF THE BENDIX CORPORATION

SQ1-51689

FINAL REPORT, CONTRACT NO. NAS8-20529

VOLUME 2

DEVELOPMENT OF A MICROMETEOROID SIMULATION DEVICE, CONSTANT AREA ACCELERATOR

7457/R1

SUBMITTED TO

GEORGE C. MARSHALL SPACE FLIGHT CENTER,
NATIONAL AERONAUTICS AND SPACE ADMINISTRATION,
HUNTSVILLE, ALABAMA, U.S.A.

24 OCTOBER 1967

PREPARED BY

J. R. B. MURPHY

SPACE SCIENCES DIVISION

COMPUTING DEVICES
OF CANADA LIMITED

AN AFFILIATE OF THE BENDIX CORPORATION

CONTENTS

CONTENTS (CONT'D)

LIST OF ILLUSTRATIONS

LIST OF ILLUSTRATIONS (CONT'D)

ACKNOWLEDGEMENTS

The author wishes to acknowledge the support provided by Mr. R.A. Barkley (mechanical design) and Messrs K.C. Hamilton and R. Lalonde (instrumentation) during this part of the program. Programming assistance for finite-difference gasdynamic solutions was provided by Mr. L.K. Badhwar, and Mr. T.L. Rollins assisted with the analytical work.

ABSTRACT

The theoretical and experimental investigation of an accelerator mounted on the muzzle of a light gas gun is described. The accelerator operates on gasgynamic principles and uses the energy and momentum of a primary projectile, launched by the light gas gun, to achieve high velocities of a relatively light secondary projectile accelerated from rest in the accelerator. The internal cross section area of the accelerator is constant and identical to that of the light gas gun barrel.

The theoretical investigation indicated that secondary velocities which were 60 to 80 percent higher than the primary velocity could be achieved for primary to secondary projectile mass ratios equal to 20 or above. It was found that such increases are independent of primary velocity, if losses are neglected.

The experimental firings gave good agreement with theory. Secondary velocities were 45 to 60 percent higher than primary velocities for a projectile mass ratio of 18. It was found that there was little tendency for the percentage increases to fall off with increasing primary velocity, indicating that energy loss effects were not severely limiting the accelerator performance.

Secondary velocities were found to be limited by anomalous failures of the disk-like metal secondary projectiles which were employed. These failures prevented the investigation of projectile mass ratios above 18 and limited the secondary velocity of the present accelerator configuration to slightly above 30,000 feet/second, for primary velocities slightly below 20,000 feet/second.

SECTION 1

INTRODUCTION

The design and development of the micrometeoroid simulation facility were described in Volume 1 of this report (Reference 1). The facility was developed with the aim of achieving velocities in the range 20,000 feet/second to 50,000 feet/second, with particles whose size may be controlled over a wide range, and whose mass can be determined in flight just prior to impact. The facility consists of a 0.5 inch light gas gun; an accelerator at the muzzle of the light gas gun to provide an improved velocity capability; and a range tank containing diagnostic equipment, including flash X-ray for mass determination in flight. The theory and the experimental application of a novel technique for in-flight mass measurement by means of X-ray photography were described in Volume 1.

The light gas gun was designed with ease of operation as a primary consideration, and the accelerator was designed to be a relatively inexpensive item, disposable after each firing. The facility was limited in length by the dimensions of the building for its accommodation at Marshall Space Flight Center. This led to the choice of a relatively short light gas gun, and a short range tank having a total length of about five feet.

The accelerator considered in Volume 1 was effectively a third stage of the light gas gun, incorporating a further reduction in area to a small diameter launch tube, and operating on a principle similar to that of the light gas gun second stage except that destructively high pressures were permitted in the accelerator compression tube. It was calculated that expansion of the compression tube walls would be of sufficiently long duration so as not to interfere with the acceleration of the secondary projectile in the launch tube. Some mass loss of the secondary projectile during launch was anticipated, which led to the provision for in-flight mass measurement.

The accelerator did not achieve the anticipated performance level, and it was concluded in Volume 1 that this was due to severe energy loss effects not included in performance computations. The losses were associated with the reduction in area from the 0.5 inch diameter compression tube to the 0.062 inch launch tube. It was therefore proposed in Volume 1, that an accelerator design be considered having no area reduction to the launch tube, and described as a "constant area accelerator". It was suggested that because of the forward velocity imparted to the gas column in the accelerator, such an arrangement would overcome severe loss effects.

The present Volume describes a theoretical and experimental investigation of the constant area accelerator. The experiments were performed on a temporary installation of the micrometeoroid simulation facility at ComDev, before delivery to the Marshall Space Flight Center. The experimental program is regarded as preliminary in nature, because of its short duration of only four months.

SECTION 2

THEORY OF THE ACCELERATOR

2.1 ADVANTAGE OF THE CONSTANT AREA CONCEPT

The constant area accelerator is illustrated in the sketch below.

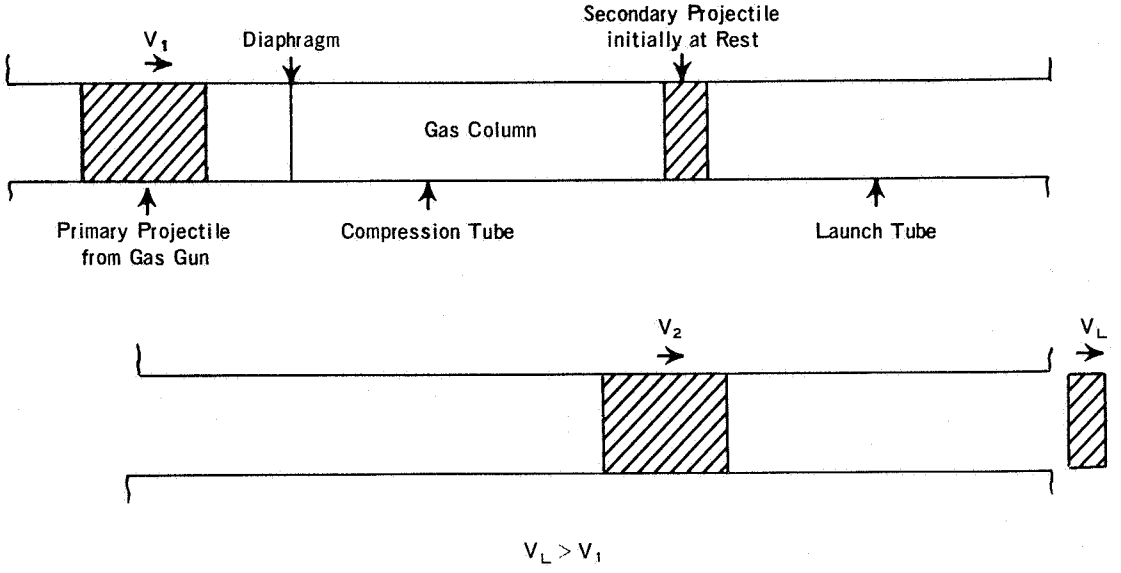

Initially the column of gas in the compression tube is at rest. A high velocity primary projectile enters the compression tube and loses energy to the gas, causing it to accelerate. Increased gas pressures force the low mass secondary projectile to accelerate down the launch tube. This exchange of energy and momentum continues to the point where no further significant decrease in the velocity of the primary projectile, or increase in the velocity of the secondary projectile, is obtained.

The constant area accelerator differs markedly from the form of the accelerator considered in Reference 1. It is important to underscore this difference. The earlier accelerator is sketched on the following page. In this arrangement, the loading gas was compressed to a high pressure reservoir having a very high escape speed. Gas expanded from this reservoir into the launch tube to accelerate the projectile. The pressures and temperatures in the reservoir will be much higher than those experienced in the launch tube, where internal energy of the gas has been

exchanged for high kinetic energies of both the gas and the secondary projectile. The process of conversion of gas internal energy into kinetic energy, as the gas expands into the launch tube, is highly dependent on losses, such as contamination due to erosion of material at the launch tube entrance, and by boundary layer friction in the small diameter launch tube. It was found in Reference 1 that such losses severely limited the accelerator performance.

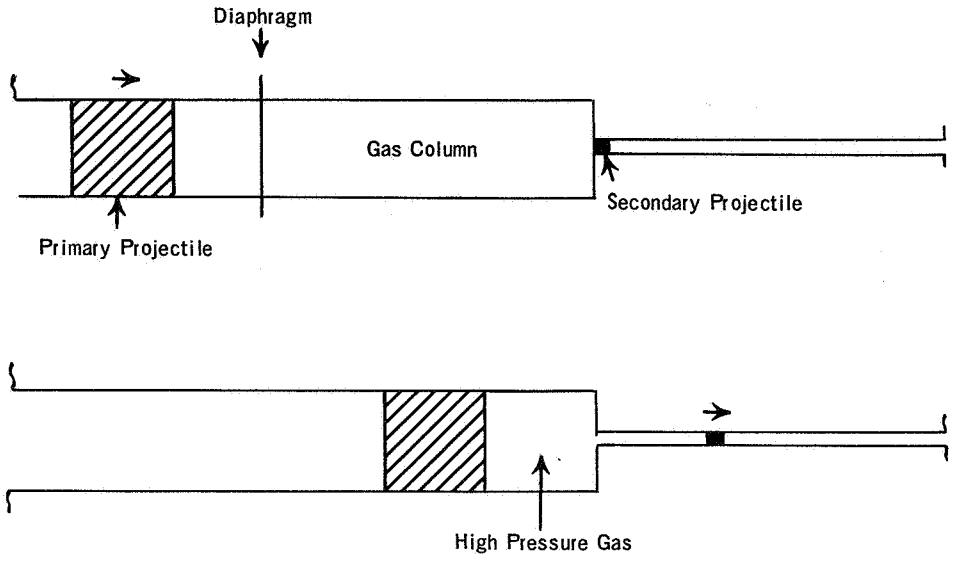

The constant area accelerator does not employ a stationary gas reservoir of high internal energy. The gas acquires kinetic energy, as well as a certain amount of internal energy, as the primary projectile continues to do work on it. The gas transfers part of its acquired energy to provide kinetic energy of the secondary projectile. Pressures and temperatures are relatively low; in fact conditions may be found such that the maximum base pressure experienced by the projectile is the highest pressure encountered in the accelerator. Because of the elimination of the high pressure gas reservoir, it was considered that the constant area accelerator would not be severely restricted in performance because of losses.

Two versions of this concept have been studied. The first is the "single-gas accelerator" in which the gas column separating the primary and secondary projectiles consists of a single homogeneous gas. The second is the "two-gas accelerator", in which the gas column initially consists of two compartments containing different gases which have differing densities. The analysis of the single-gas and two-gas accelerator is discussed in the following sections.

2.2 SINGLE-GAS ACCELERATOR

2.2.1 SIMPLIFIED ANALYSIS

An approximation to the accelerator performance may be obtained if it is assumed that the acceleration process is a collision process involving the primary projectile, the gas and the secondary projectile. Conditions at the end of the acceleration process may be related to the mass and velocity of the primary projectile by simple equations of conservation of momentum and energy. Computer runs, in which the detailed gas dynamic processes are calculated, have shown that towards the end of the acceleration process the gas density becomes uniform and the gas velocity linear between V_a and V_L (see Section 2.2.2). This fact greatly simplifies the solution of the conservation equations.

The equations for the single-gas accelerator are given in Appendix A. It is interesting to note that the velocity multiplication factor V_L/V_1, depends only on the relative masses of the primary projectile, the gas, and the secondary projectile; and on the factor 'K' which is introduced to express kinetic energy losses in the system. For example, K = 1.0 means that there is no loss of kinetic energy in the system; K = 1.5 means that an amount of energy is absorbed in the gas which is equal to 50 percent of the gas kinetic energy.

Figure 1 shows the variation of the velocity multiplication factor V_L/V_1 for the case of K = 1.0 and the case of K = 1.65. The curves are plotted for values of M_P/M_L (primary projectile mass divided by secondary projectile mass) varied between 5.0 and 40. The inclusion of the loss factor 1.65 reduces the performance considerably and changes the shape of the curves so that peak performance is achieved at low values of M_G/M_L (gas mass divided by secondary projectile mass).

The value K = 1.65 was based on the internal energy remaining in the gas in typical gasdynamic computer runs. It was found from these computer runs that the factor 'K' varied over a wide range depending upon the accelerator conditions. This characteristic is discussed in the next section.

2.2.2 GASDYNAMIC ANALYSIS

The above simplified analysis showed that initial and final conditions in the accelerator may be related with relative ease. The end conditions may also be calculated by considering the unsteady compression and expansion processes which take place in the gas. To do this a computer program was written which solves the partial differential equations of unsteady

motion of the gas by a numerical finite-difference method. This program is described in Section 2.4. The program can handle shock waves automatically and was extensively tested for accuracy.

The simplified analysis indicated that for similar gas and projectile mass, similar accelerator performance would be expected, regardless of gas characteristics. The first application of the single-gas computer program was to investigate performance when gases having different molecular weights are employed. Computer runs were made for cases having identical masses of gas and projectiles, and identical primary projectile velocity (25,000 feet/second). The accelerator geometry was the same for each run. Final projectile velocities were as follows:

Helium	35,480 feet/second
Argon	35,320 feet/second
Hydrogen	34,140 feet/second

Thus performance is little affected by varying molecular weight between 2 and 40.

The reason for the above similarity stems from the fact that the compression and acceleration of the gas is produced by a very strong shock process. The primary projectile drives a very strong shock wave into the gas which reflects from the projectile base. Multiple reflections may occur between the primary and secondary projectiles before the process subsides to a quasi-steady condition. Consider the reflection of the first shock wave, as shown in the sketch below.

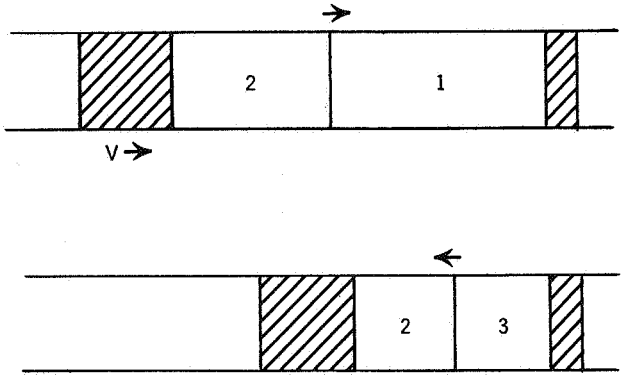

If the secondary projectile were to remain stationary, strong shock relationships for an ideal gas would give the following expressions for the conditions in region (3).

density $\rho_3 = \left(\frac{\gamma+1}{\gamma-1}\right)^3 \rho_1$

pressure $p_3 = \frac{V^2}{2} \frac{(\gamma+1)^2}{(\gamma-1)} \rho_1$

where p_3 = gas pressure in region (3)

γ = ratio of specific heats

ρ_1 = loading gas density

ρ_3 = gas density in region (3)

Pressure and density are thus independent of the gas molecular weight and depend only on γ and the loading density (or mass for fixed geometry). As the projectile commences to accelerate, the pressure decay on its base will be governed by the sound speed and the escape speed in the region (3). It is easy to show that these quantities depend only on γ. Thus, because of the strong shock processes, it would be expected that gases having similar γ will give similar performance in a given accelerator. This explains the similarity between the results for helium and argon above. The small difference in muzzle velocity is probably caused by the difference in the initial specific internal energy of each gas. In practice operation with argon would be much hotter than with helium, which would give rise to increased losses.

A distance-time diagram for the helium case is shown in Figure 2. The overall length of the accelerator was 1.0 foot. Figure 3 shows the velocity and density distributions in the gas when the secondary projectile is at the muzzle, and indicates that conditions are approaching the constant density and linear velocity profiles assumed in the simplified analysis. It was found that performance agreed well with the appropriate kinematic calculations having the same value of the factor K. This factor varied between 1.61 and 1.68 in the above gasdynamic runs, due to residual internal energy in the gas.

Attention was then turned to applying the gasdynamic computer program to the investigation and optimization of the theoretical performance of the accelerator. In order to make maximum use of the simplified analysis to establish trends and save computer time, it was necessary to establish a criterion for the basis on which to compare calculated accelerator performance. To explain this, let us consider the later stages of the acceleration process when the gas density is fairly uniform and the situation compares well with the simplified analysis for the same value of the factor 'K'. The

secondary projectile will continue to gradually accelerate while the gas continues to lose internal energy (reducing the factor 'K'). In some cases it might be worthwhile to lengthen the launch tube to take advantage of the continuing acceleration, in other cases the acceleration is too gradual to make it worthwhile. To tackle this problem two fairly arbitrary criteria were established.

(a) The first criterion is to compare all accelerators on the basis of having the same geometry (i.e. having the same ratio of launch tube length to loading tube length). For this case it was assumed that the launch tube length is equal to the loading tube length.

(b) The second criterion is to compare accelerators having launch tubes long enough so that any additional length does not provide worthwhile gains in performance. It was arbitrarily assumed that the muzzle of the accelerators would be at the point where the velocity gain in the final 10 percent of launch tube length is only between 1.0 and 1.5 percent (usually 1.3 percent).

These criteria will be referred to as criterion (a) and criterion (b).

One of the first tasks was to study further the correlation between the simplified analysis and results obtained from detailed gasdynamic computer calculations. It was found, for calculations made at projectile mass ratios (M_P/M_L) of 5, 10, 40 and 500, that good correlation was in fact obtained. Figure 4 shows the multiplication factors achieved in a series of calculations for a projectile mass ratio of 10, in which the criterion (b) was employed. It can be seen that the value of 'K' obtained in the computations decreases as the ratio of gas mass to secondary projectile mass M_G/M_L is increased. This causes the computed multiplication factors V_L/V_1 to fall on a line which traverses the simplified results for fixed values of 'K'.

Associated with the above task was the problem of establishing whether the gas dynamics results are themselves consistent in cases having the same values of M_P/M_L and M_G/M_L, but in which the primary projectile velocity, the masses involved, the type of gas involved and the scale may be physically different. It was found that, provided primary projectile velocity was high enough to cause strong shocks, the correlation was very good. For example, in Figure 4 there are two computed points at $M_G/M_L = 3$. These have almost identical values of 'K' and multiplication factor, but are

for primary projectile velocities of 14,000 feet/second and 25,000 feet/second. Similar correlation was found in varying the scale, type of gas and the masses involved*.

The above results indicated that maximum advantage should be taken of the simplified analysis at the appropriate 'K' to assist the analysis of accelerator performance. The variation of 'K' with M_G/M_L, from gasdynamic computer runs, is shown in Figure 5 for criterion (a) and in Figure 6 for criterion (b). In every case there is a tendency for 'K' to be reduced for increasing M_G/M_L, and it is interesting to observe that each value of M_P/M_L possesses a distinct curve. These curves have been used to help produce performance curves for both criterion (a) and criterion (b), by using these values of 'K' in the simplified analysis. Figure 7 shows the multiplication factors achieved under criterion (a) while Figure 8 shows those for criterion (b). The accelerator geometry which is required to achieve criterion (b) is shown in Figure 9. The required lengths were found to fall close to a single curve as a function of M_G/M_L only, for all computer runs. Constant geometry is represented by a horizontal line at unity on Figure 9; thus the performance of the constant geometry accelerator will be lower than for the case of criterion (b), for M_G/M_L higher than approximately 1.0.

The next task was to determine suitable conditions for accelerator operation from the standpoint of both performance and ease of launching. A glance at Figure 8 for example shows that for $M_P/M_L = 40$, highest performance is predicted at $M_G/M_L = 3$, while for $M_P/M_L = 10$, highest performance is predicted at very low values of M_G/M_L. However, the curves tell nothing of the shock wave structure and the resulting base pressures to which the secondary projectile will be subjected. The gas dynamic computer runs have been made for a wide variety of conditions of geometry, incoming velocity, etc. which were found to correlate well with one another in terms of non-dimensionalized performance. The existence of a similar correlation in base pressures was suspected because of the characteristics of strong shock waves which were mentioned previously. These characteristics suggested that the base pressures for all computer runs could be approximately reduced to a common standard geometry, secondary projectile mass and primary projectile velocity. The upper curve of Figure 10 shows the results standardized to a compression tube length of six inches, secondary projectile weight of 1.0 gram and primary velocity of 25,000 feet/second.

* These results could have been presumed in advance were it not for real gas effects

The shape of this curve can be explained by reference to the shock histories in the accelerator and their influence on the secondary projectile base pressure. Base pressure histories at $M_G/M_L = 1.0$, for example, are shown in Figure 11. The base pressure is characterized by two peaks, corresponding to the arrival of shock waves. The first peak is the stronger and gives rise to the peak base pressure. If the ratio of M_G/M_L is increased above 1.0, the first shock becomes stronger, because of the increased gas density, whereas the second peak becomes progressively weaker. On the other hand, as M_G/M_L is reduced below one, the first shock becomes weaker while the second becomes the stronger. Eventually the second shock wave is surpassed in strength by the third shock wave as M_G/M_L is reduced. Figure 12 indicates schematically the shape of the base pressure curves for values of M_G/M_L between 0.3 and 3.0. At values of M_G/M_L below about 0.25 the third shock wave rapidly becomes very strong. Thus for a given secondary projectile mass there appears to be an optimum choice for the gas mass in the neighbourhood of $M_G/M_L = 0.3$ to 0.8, from the standpoint of minimizing peak projectile pressure.

2.3 TWO–GAS ACCELERATOR

In the two-gas accelerator the loading tube is divided into two compartments containing gas so that the gas in the compartment adjacent to the primary projectile has a higher density than that in the second compartment. The underlying concept is that this density discontinuity will be retained when uniform conditions are reached, as indicated in the sketch below.

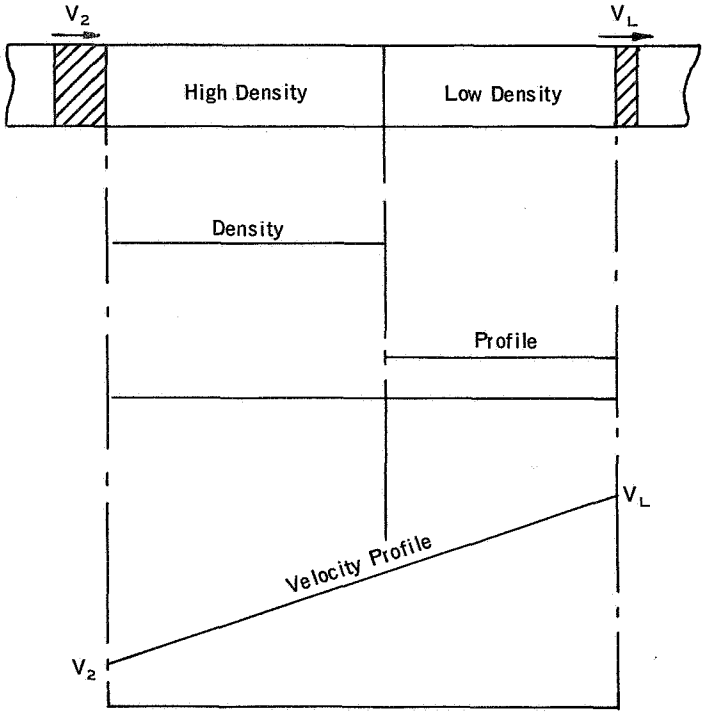

FINAL CONDITIONS

Thus for a given mass of gas and a given velocity profile V_2 to V_L, the energy and momentum absorbed by the gas will be less than for the case of uniform density. This leads to the possibility of improving accelerator performance over the single-gas case.

2.3.1 SIMPLIFIED ANALYSIS

Simple conservation relationships may be used to relate the stage when uniform conditions have been reached, to the initial primary projectile velocity and mass. These relationships make use of the factor 'K' to describe loss of kinetic energy as internal energy of the gas or as heat loss. The relationships are given in the Appendix B. Figure 13 shows a sample plot of velocity multiplication factor for the case where the final density ratio is equal to three, the value of 'K' is equal to 1.5, and for which the final position of the density discontinuity is situated at distances of 0.5 and 0.7 times the gas column length (measured from the primary projectile).

Two problems have arisen in analytical studies for the two-gas case. The first is associated with the fact that there are two additional parameters to be considered: the density ratio and the position of the density discontinuity or interface. Not only do the additional variables complicate the analysis considerably, but there is also the more difficult problem that the interface position and density ratio change as the acceleration process proceeds, so that the final values are normally considerably different from the initial values. Thus, for example, an initial density ratio of 10:1 and an interface position of 0.5 has been found to alter to values of 3:1 and 0.79 in one case, and to 5:1 and 0.66 in another, in gasdynamic computations. The only differences between these runs were alterations to the value of M_G/M_L and to the gas mass itself. It does not seem possible to predict the final values accurately, and it is only the final values which are of interest for the simplified analysis. The other problem is that it takes much longer for conditions to become uniform than in the case of the single-gas accelerator. Computer runs have indicated that normally conditions are still non-uniform at the point where the further acceleration of the secondary projectile is becoming insignificant, at values of projectile travel which are large compared with the compression tube size. It was necessary to decide if it was worthwhile to expend considerably more computer time simply to bring conditions to the point where valid comparisons with the simplified analysis may be made.

Because of these problems it was decided to make comparisons of the two-gas accelerator on the basis of constant geometry only. The chosen geometry was the case of launch tube length equal to compression tube length. This unfortunately meant that direct comparisons with the simplified analysis could not be made, although the latter could be used to provide guidance.

2.3.2 GASDYNAMIC ANALYSIS

The single-gas computer program was modified to treat the two-gas case. Dissimilar gases with the associated contact discontinuity may be handled. The program is described in Section 2.4.

Most runs have been made for the case of projectile mass ratio $M_P/M_L = 10.0$. The runs have been used to probe the effects of altering the initial density ratio and the interface position at values of M_G/M_L of 0.5, 1.0, 3.0, 4.0 and 5.0. Detailed results will not be presented in this report because no clear trends emerged and in particular no significant performance advantage over the single-gas case was observed. The best velocity multiplication factors have been values of 1.75 for the cases $M_G/M_L = 4.0$ and $M_G/M_L = 5.0$ with an initial density ratio of 40 and an initial interface position of 0.2. These results are shown in Figure 14, together with some results for an initial density ratio of 10.0. Figure 14 also shows the results of computer runs at $M_P/M_L = 18.0$, which was the value used for experimental firings.

The most significant result of the two-gas computations was the role played by the lower density gas as a shock wave attenuator. This is illustrated by the simplified distance-time diagram sketched below, in which expansions have been omitted.

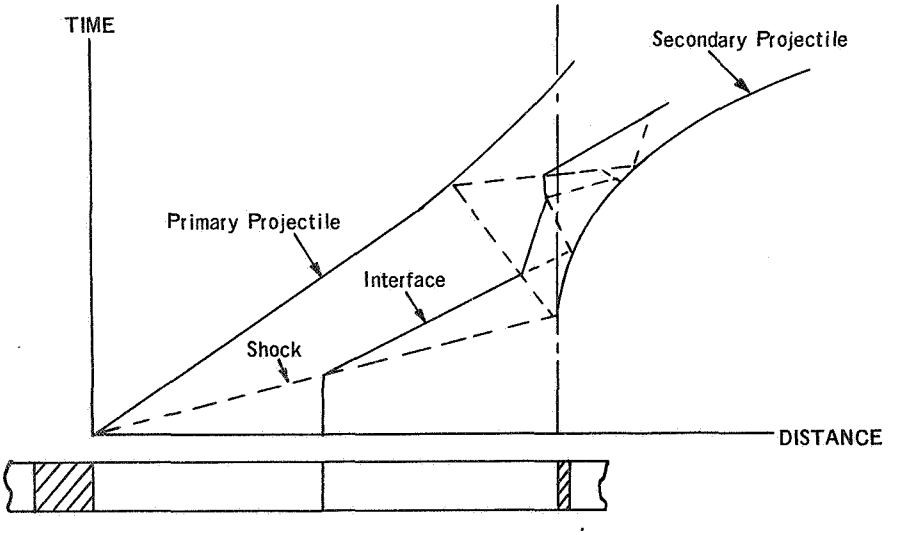

The strength of the initial shock wave is reduced as it is transmitted into the lower density gas. This shock may undergo reflections between the secondary projectile base and the gas interface as well as transmitting a reflected shock back into the higher density gas towards the primary projectile face. The net result is that the secondary projectile experiences a series of weaker shock waves compared with the two or three strong shock

waves experienced in the case of the single-gas accelerator. Much lower peak base pressures were observed in two-gas computations compared with the single-gas case. On the other hand, peak front face pressures at the primary projectile were higher, than in the single-gas case. The lower curve of Figure 10 shows typical base pressures computed for the two-gas accelerator, for a projectile mass ratio M_P/M_L equal to ten, and for a gas mass ratio M_A/M_B of ten. Two points are also given at M_A/M_B equal to 15, indicating that still greater reductions are possible by increasing the value of M_A/M_P. In the limit this would lead to a vacuum in the second gas compartment, and this possibility is discussed further in Section 3.3.1.

2.4 COMPUTATION METHODS

Computer programs were written to calculate the unsteady gas-dynamic operating cycles of the single-gas and two-gas accelerators. These programs were based on methods developed at ComDev for the calculation of the interior ballistics of light gas guns and conventional guns (Reference 2).

In these programs one-dimensional particle-differential equations describing the conservation of mass, momentum and energy are written in finite-difference form in the Eulerian reference frame. These, together with the gas equation-of-state, are used to calculate complete solutions of the flow and the projectile motions at successive small time intervals. The accelerator is divided into a large number of spatial intervals, in each of which the gas properties are calculated.

The finite-difference method was carefully tested for its ability to handle accurately the automatic calculation of shock waves. In addition, the two-gas program is provided with a means for accurately calculating the interface between the two gas columns. The latter may differ from one another in any desired manner, including the type of gas and the equation-of-state used to describe each gas. This technique, which is not common in Eulerian methods, is described in Reference 3. The programs were thoroughly tested for accuracy and for the conservation of the system momentum and energy. The two-gas program was initially tested by performing shock tube calculations for cases in which the driver and driven gases were dissimilar.

The equation-of-state allows for molecular co-volume effects and their variation with the specific local internal energy of the gas. This is discussed in more detail in Volume 1 of this report (Reference 1).

SECTION 3

EXPERIMENTS

3.1 INTRODUCTION

For the development program reported here, the facility was temporarily installed in a range building at the Space Sciences Division of ComDev. A total of 79 firings was made, of which 64 were accelerator development firings. The accelerator firings took place over a period of approximately four months (December 1966 to March 1967). Figures 15 and 16 are photographs of the launcher installation at ComDev, and Figure 17 shows a schematic diagram of the light gas gun, accelerator and range tank. The configuration of the accelerator and its attachment to the muzzle of the light gas gun is depicted in Figure 18.

The conditions and results of the firings are summarized in Table 1, Sheets 1 to 4. The firing numbers refer to ComDev designations. A detailed chronological history of each firing is not given here. Instead, a brief historical sketch of the firing program is given, followed by descriptions of the observed trends and the experiments made to investigate these trends. Further analytical studies were made in the light of experimental observations; these studies are described in Section 4.

3.2 OUTLINE OF FIRING PROGRAM

The initial series of firings up to firing No. 633 was made to determine the most suitable light gas gun operating conditions, to investigate the capability of the primary projectile to shear the diaphragm at the accelerator entrance without seriously damaging itself, and to establish the most suitable arrangement of the flash X-ray set up. The following gun loading conditions were retained throughout subsequent firings:

piston mass	1300 gm
gas loading (hydrogen)	95 lb/in^2 abs.
primary projectile mass	4.0 gm

Charge weight was varied to obtain the desired primary projectile velocity.

Initial accelerator firings (616 and 619) employed plastic secondary projectiles having length to diameter (L/D) ratios of 0.4. Polycarbonate and nylon projectiles were chosen because these materials are known to have good resistance to rapidly applied dynamic stresses. Break up of

these projectiles was observed, and plastic projectiles were discarded in favour of short disk-like metal projectiles for the reasons given in Section 4.4. The positioning of the X-ray heads, shown in Figure 15, proved unsuitable for photographing the short disk-like projectiles due to lack of contrast, and the set up was revised after firing 632.

The X-ray arrangement adopted after firing 632 is shown in the sketch below. A block diagram of the instrumentation is shown in Figure 19 (see also Figure 17).

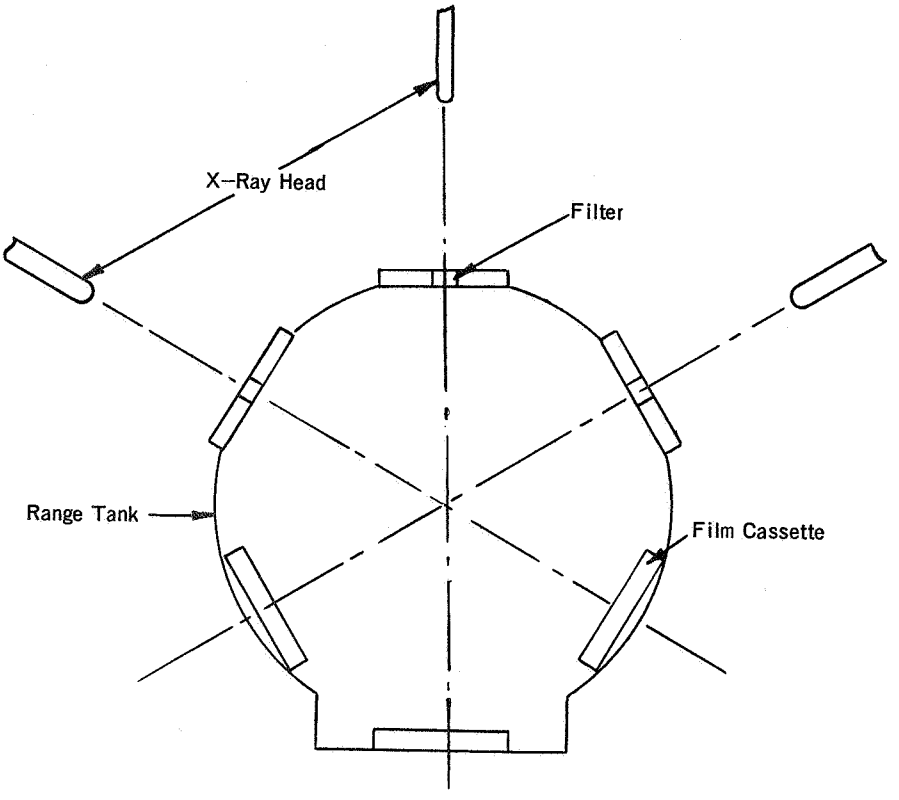

The X-ray heads were mounted in a plane at right angles to the line of flight and were pulsed consecutively, according to pre-set delays triggered by the interrupted-beam muzzle detector. The X-ray voltage and the filter were chosen for optimum contrast over a range of possible projectile material and thicknesses. In addition each strip of film in the cassette was exposed only once, which further aided contrast. Back up signals to aid in the accurate determination of projectile velocities were provided by a paper chronocard detector, which was mounted on the downrange side of a thin replaceable aluminum bulkhead so that no signal was possible until the bulkhead was perforated by the projectile; and by a light detecting diode viewing the target area which provided a history of the light intensity caused by the impact on the target.

Good X-ray results were obtained in firings 634 to 637, as shown in Figures 20 to 23. These firings employed aluminum projectiles whose L/D ratio was 0.05, and which weighed 0.22 gm. The mass of helium gas in the accelerator was chosen so that $M_G/M_L = 0.35$. Analytical work suggested that this value would minimize the peak base pressures experienced by the projectile, as shown in Figure 10. The compression tube of the accelerator was 4.75 inches long; and the launch tube was 4.5 inches long. Good performance was obtained, in that, although the primary velocity was increased steadily from 11,800 feet/second to 17,750 feet/second, the secondary velocity was consistently about 50 percent higher, giving a near-constant velocity multiplication factor of 1.5. Failure of the secondary projectile occurred in firing 638; gouging of the compression tube wall at the accelerator entrance and severe damage to the primary projectile was also observed on this firing. At the time it was not clear whether or not the gouging damage had contributed to the failure of the secondary projectile.

Accelerator theory stated that the velocity multiplication factor would be improved by increasing the projectile mass ratio M_P/M_L. It was not practicable to increase the primary projectile mass, and so the mass of the secondary projectile was reduced by using shorter aluminum disks. Projectiles having L/D ratios of 0.025 to 0.040 were employed without success in firings 642, 643 and 646. At later stages of the program, as improvements were made to the operating cycle of the accelerator, projectiles having an L/D ratio of 0.025 were fired from time to time but intact projectiles were never achieved. Possible reasons for these failures are discussed in Section 4.3

For firing 648 a longer compression tube was introduced. This compression tube was about twice as long as that used in previous firings, and measured 8.4 inches (the launch tube length was not altered). The purpose of this change was to lower the peak pressures experienced by the secondary projectile. Accelerator analysis showed that pressures in the accelerator are approximately inversely proportional to the compression tube length. It was thus possible to determine if a reduction in base pressures would enable the accelerator performance to be extended beyond that achieved in firing 637. In fact little success was obtained, and, as discussed in Section 4.1, it was realized that this might be due to the fact that the peak base pressure was being experienced by the secondary projectile after it had moved some distance down the launch tube, by which time it might have become slightly misaligned. It was thought that the arrival of a strong shock wave at this point might tend to drive the secondary projectile against the launch tube wall causing it to break up. To investigate this hypothesis experimentally two approaches were adopted:

APPROACH (a). Employ conditions in the single-gas accelerator so that high base pressures are experienced by the secondary projectile only at the start of projectile motion.

APPROACH (b). Use the concept of the two-gas accelerator to develop an operating cycle in which relatively low base pressures are maintained throughout the projectile travel.

Approach (a) and Approach (b) are discussed further in Section 4.1.

APPROACH (a). Approach (a) led to the choice of a mass of loading gas which satisfied the ratio

$$\frac{M_G}{M_L} = 0.8$$

Initial firings gave multiplication factors which were surprisingly low, although the secondary projectile was in excellent condition in each case. At first it was thought that this was caused by heat loss from the gas, but replacement of the helium by much cooler hydrogen gas gave the same result. It was eventually found that gasdynamic computer runs had underestimated the required launch tube length. The launch tube length was therefore increased to about 9.0 inches; this necessitated lengthening the dump tank to accommodate the larger accelerator. The longer launch tube enables a velocity multiplication of over 1.5 to be achieved, as anticipated; secondary velocity increased to over 29,000 feet/second (firing 676).

During the above firings, it was decided to introduce a small amount of hydrogen into the barrel of the light gas gun in an attempt to eliminate gouging at the accelerator entrance, which had continued to be a problem. The reasons for this choice are given in Section 4.4. Hydrogen at a pressure of 75 mm of mercury was admitted to the evacuated and sealed barrel. Adoption of this measure completely eliminated gouging and was used on all single-gas accelerator firings after 652. The use of a contoured front face on the primary projectile was also shelved when the elimination of gouging had been established. It was found that a simple flat faced cylindrical shape performed well and had good resistance to break-up.

Extension of the performance to higher velocities, by increasing primary projectile velocity, was hampered by the appearance of difficulties with projectile release. On some firings it was noticed that secondary projectile failure was accompanied by slight damage at the entrance to the launch

tube, indicating that the projectile had sheared improperly. A number of firings were therefore devoted to studying the most suitable shear mechanism for releasing the projectile. These firings, described in Section 3.3.3, led to the choice of a partially cut shear flange, as sketched below.

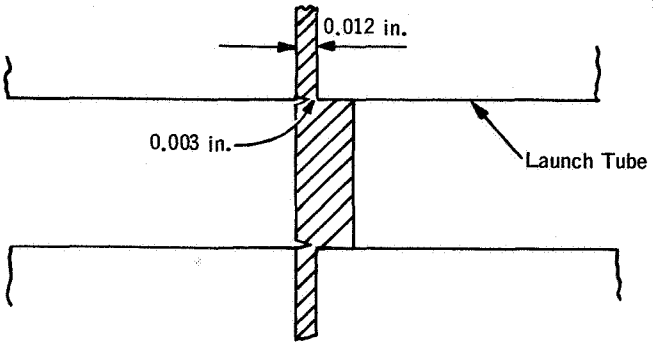

During the release tests an interesting result was incidentally achieved when investigating the method sketched below, in which a thin Mylar diaphragm supported the gas pressure and the projectile was positioned against it on the gas loading side.

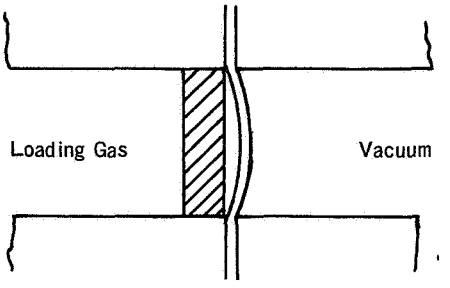

This method was employed because of the difficulty of obtaining a strong bond between Mylar and aluminum. In theory the method provided a means of ensuring that the projectile was undeflected by the loading gas, thus presenting a plane surface at the arrival of the first and strongest shock wave. The desirability of this state of affairs is discussed in Section 4.3. In the firing the projectile was observed to have broken into small fragments having very low velocity. The Mylar diaphragm was observed on one X-ray, apparently intact and travelling well in front of the secondary projectile debris. The time between picture and the impact chronograph signal gave the Mylar diaphragm a velocity approaching 55,000 feet/second.

As was mentioned earlier, from time to time firings were made with the shorter 0.025 inch aluminum projectile, to determine if increased velocity multiplication could be achieved by increasing the projectile mass ratio

M_p/M_L (from about 18.0 to approximately 35.0). Intact secondary projectiles were not achieved, which appeared surprising in view of the relatively low base pressures experienced by this projectile (see Section 3.3.4). Because of this, two firings were made employing longer aluminum projectiles having L/D ratios of 0.08 and 0.1. The purpose was to see if there was a trend of increasing base pressure capability with increasing projectile length; and if, as a result, increased length would lead to a better chance of achieving high performance quickly. Intact projectiles were achieved, but velocity multiplication was relatively lower than for the normally used projectile (L/D = 0.05), as anticipated. The peak pressure sustained by the projectiles was relatively high; being over 700,000 lb/in^2 in one case, or nearly twice the value at which the normally-used projectile had been observed to break up. This lent strong support to the view that pressure alone is not the major factor causing damage, and that there must be some additional mechanism to account for the failure of the shorter projectiles at relatively lower peak base pressures.

In order to increase projectile length while retaining the projectile mass ratio of 18.0, magnesium projectiles were constructed having a value of L/D equal to 0.08. Only a few firings were possible before the firing program was terminated, at which time performance was similar to that achieved by the normally-used aluminum projectile in that muzzle velocities up to and slightly exceeding 30,000 feet/second, with velocity multiplication factors of about 1.5, were achieved.

The validity of Approach (a) was tested from time to time during the firing program. This was done because it was felt that the trends observed earlier in the program might have become invalid as improvements, such as the optimization of projectile release, were incorporated. Values of M_G/M_L, which were used, ranged between 0.15 and 0.4. In every case secondary projectile break-up resulted, and it was concluded that the approach was valid.

APPROACH (b). Due to the time scale of the program only a few firings were possible for the investigation of Approach (b). Two-gas accelerator firings utilized the barrel of the light gas gun as the accelerator compression tube, as described in Section 3.3.8. Only five firings were made, which were insufficient to determine satisfactory operating conditions.

3.3 DESCRIPTION OF OBSERVED TRENDS

By far the majority of accelerator firings employed the single-gas accelerator concept; only five two-gas accelerator firings were made.

The following subsections refer to single-gas firings, with the exception of Section 3.3.8.

3.3.1 CHOICE OF PARAMETERS M_P/M_L, M_G/M_L

The mass of the primary projectile, M_P, was chosen as the heaviest mass which could conveniently be launched by the light gas gun to a velocity of 20,000 feet/second or slightly above. For most firings, M_P/M_L was chosen as close to 20 as possible, as accelerator theory indicated that good performance should result at this value. The actual value used (approximately 18.0) resulted from the use of a stock aluminum sheet size when manufacturing the disk-like aluminum projectile.

No quantitative experimental trend was observed for the dependence of accelerator performance on variations in M_P/M_L. A performance drop was however observed when M_P/M_L was reduced to 11.0 in firing 695; the velocity multiplication factor dropped to 1.23 compared with a value of about 1.5 at $M_P/M_L = 18.0$. Firings at higher values of M_P/M_L up to a value of about 35 were made employing short aluminum secondary projectiles, but broken-up projectiles were consistently observed (see Section 4.3 for a discussion of these failures).

The mass of gas, M_G, was initially chosen to satisfy the relationship

$$\frac{M_G}{M_L} = 0.35$$

This value was chosen to provide a close-to-minimum value of the peak base pressure experienced by the secondary projectile, and was taken from the theoretical curve shown in Figure 10. Good performance was achieved for primary velocities up to 17,800 feet/second (firings 634 through 637). For higher performance it was found necessary to use a value of M_G/M_L such that

$$\frac{M_G}{M_L} = 0.8$$

As described in Section 4.1, this value was chosen in order to concentrate the peak base pressure at the start of projectile travel. It was found experimentally that this permitted the launching of intact secondary projectiles for primary projectile velocities up to 20,000 feet/second.

The choice of the value $M_G/M_L = 0.8$ appeared to be valid, as attempts

were made from time to time during the firing program to achieve higher performance than that of firing 637, with the value of M_G/M_L varied between 0.15 and 0.4 (firings 645, 648, 649, 654, 657, 661, 663, 684). These firings were not successful.

3.3.2 VELOCITY MULTIPLICATION FACTOR

A critical aspect of the constant-area accelerator development has been the need to determine how the velocity multiplication factor varies as primary velocity is increased. Accelerator theory states that, in the absence of heat losses, the multiplication factor should be independent of primary velocity, however in practice one would expect that it should fall off somewhat since losses should increase as the primary velocity is increased. Figure 24 shows the observed trend for firings at $M_G/M_L = 0.35$ (firings 634 to 637) and $M_G/M_L = 0.8$ (firings 676, 681, 704, 706, 707 and 716). For almost all of these firings, which represent the highest multiplication factors which were confirmed, the values lie between 1.45 and 1.6. Over this primary velocity range there appears to be little tendency for the factors to become reduced with increasing primary velocity. This emphasizes the potential of the accelerator technique.

For firings at $M_P/M_L = 18.0$ and $M_G/M_L = 0.8$, it was found experimentally that it was necessary to increase the launch tube length, over that which was considered adequate from theoretical studies, in order to achieve satisfactory performance. Possible reasons are discussed in Section 3.4.2. The effect of launch tube length is shown in Figure 25. The results for the shorter launch tube are from firings 649, 650, 652 and 653; firings which employed the longer launch tube were 676, 681, 704, 706, 707 and 716. Further increases in launch tube length were not explored.

No variation of velocity multiplication factor with change in M_G/M_L was observed. Figure 26 shows the factors obtained in all firings at $M_P/M_L = 18.0$, in which intact secondary projectiles were achieved. Firings in which the secondary projectile was damaged, although essentially intact, are plotted with a solid circle. All the results lie below the theoretical curve, which was obtained by cross plotting the results shown in Figure 7, however the results for the longer launch tube at $M_G/M_L = 0.8$ are low in muzzle velocity by only 5 to 15 percent compared with the theoretical computations.

3.3.3 METHOD OF PROJECTILE RELEASE

A number of firings were devoted to the investigation of a number of alternative methods of projectile release. The need for such tests became

apparent when it was noticed in some firings (e.g. firing 683) that projectile release was leading to damage to the entrance of the accelerator launch tube, and apparently also was causing damage to the secondary projectile. The release tests were made on firings 693, 694, 700, 701, 704, 715, 716 and 717; and examined the following alternatives.

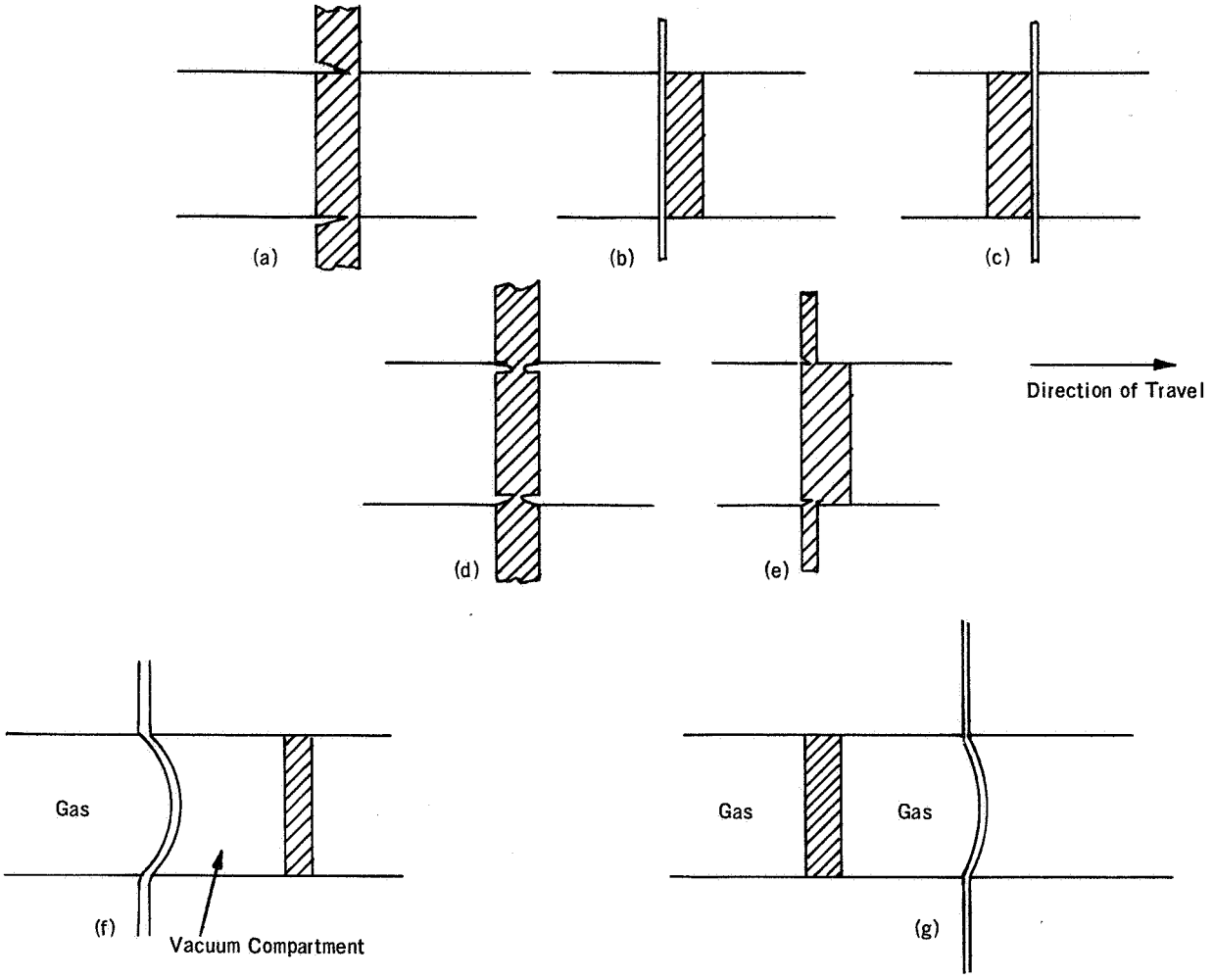

Configuration (a) was investigated for two thicknesses of residual material; 0.006 inch and 0.003 inch. Configuration (b) was tested using a thin Kapton diaphragm bonded to the aluminum, and Argon gas was employed to reduce the loading pressure to less than 60 lb/in^2. Configuration (c) utilized an unbonded Mylar diaphragm placed forward of the aluminum projectile. In configuration (d) the undercuts were dimensioned so that the sheared projectile would be somewhat less than bore size. Configuration (e) employed a thin undercut flange, so that a substantial portion of the projectile was inserted into the launch tube, thus assuring a clean entry of the front face.

In configuration (f) an evacuated compartment was employed because the loading gas and the projectile, similar to the concept considered in theoretical studies of the two-gas accelerator (Section 4.1). For the release test the compartment was for convenience made relatively short; the primary purpose was to enable the projectile to be placed freely in the launch tube and thereby avoid the initial deflection by the loading gas. A similar purpose was intended in configuration (g), however in this case the projectile was surrounded by gas at the loading pressure. It was intended that during its initial acceleration the projectile would drive a shock wave ahead of it to shear the diaphragm, thereby permitting the gas ahead of the projectile to escape. Configurations (f) and (g) were tested at the close of the firing program.

Configuration (e) proved to be the most satisfactory of the first four months. A 0.012 inch thick flange was employed, undercut to 0.003 inch on the diameter of the launch tube. An apparently successful test with (f) was made in firing 716; however further development was unfortunately not possible.

3.3.4 EFFECTS OF PROJECTILE LENGTH

Initial firings (616 and 619) employed plastic projectiles whose L/D ratio was 0.4. Fragmentation of these projectiles was observed, and consideration of the unsteady stress propagation caused by gasdynamic shock waves arriving at the base of the projectiles led to the view that the break-up was caused by a spall-like failure mechanism (see Section 4.3.1 for a discussion of this projectile failure mode). This led to the choice of short metal projectiles for subsequent firings.

There was much that was baffling about the failures which were observed of short projectiles. Typically, projectiles were launched in excellent condition as primary projectile velocity was increased, until the point was reached where a further small increment in primary velocity would cause severe damage to the secondary projectile. In other words, the condition causing failure was reached abruptly, without any indication of increasing projectile deformity as the condition was approached. Another phenomenon which was observed in X-ray photographs was that most intact projectiles were slightly "dished" in shape, and normally were dished so as to be concave on the front face, which is the reverse of that which would have been anticipated assuming that the projectile had been subjected to wall friction. Furthermore, it was found that there was a strong dependency between the peak base pressures at which projectile failures occurred, and the length of the projectile. The shortest projectiles fired (L/D = 0.025) were unsuccessful even though their peak base pressures were relatively low (150,000 lb/in^2 or lower). At the other extreme, the longest disk-like

projectiles (L/D = 0.1) were able to withstand a peak base pressure in the neighbourhood of 750,000 lb/in^2. This dependency is depicted in Figure 27. The upper point on this curve is taken from results mentioned by Moore for magnesium-lithium alloy (Reference 4).

Possible reasons for the above anomalies are discussed in Section 4.3.2.

3.3.5 ELIMINATION OF ACCELERATOR GOUGING

The earlier accelerator firings were troubled by gouging of the compression tube material at the accelerator entrance; apparently caused by a combination of high temperatures and pressures when the Mylar diaphragm was ruptured by the primary projectile (see Section 4.4). A small amount of hydrogen gas was introduced into the barrel of the light gas gun in firing 653, as indicated in the sketch:

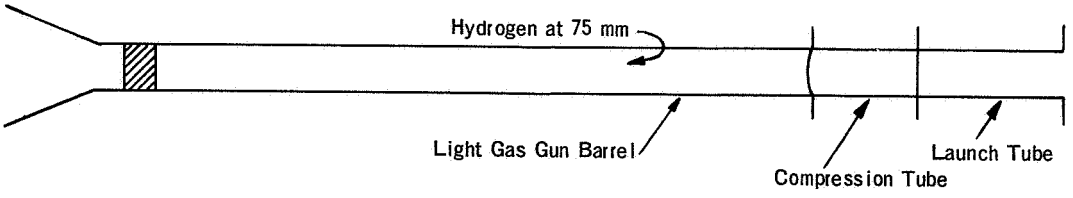

The mass of hydrogen was negligible compared with the mass of the accelerator loading gas. This procedure was found to eliminate the gouging problem and was used on subsequent firings.

3.3.6 ACCELERATOR GEOMETRY

Two firings, 664 and 670, utilized the barrel of the light gas gun as the compression tube of the accelerator, as shown in the sketch below.

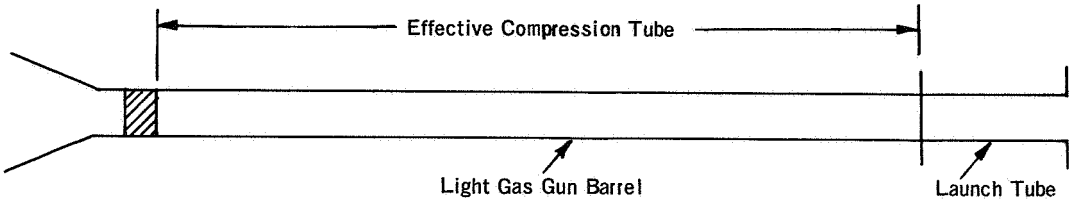

As explained in Section 4.5, the main intention was to reduce the severity of shock waves which are transmitted to the projectile base. Pre-trigger of the muzzle-detector in each case prevented a positive velocity measurement, however it appeared that the performance was low. The highest performances were achieved with the accelerator geometry indicated in the following sketch.

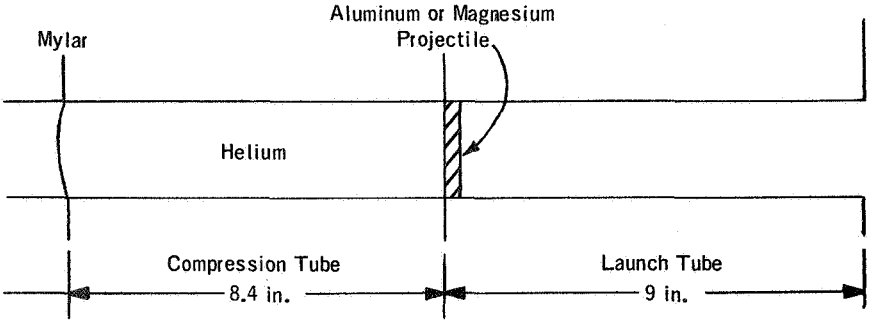

3.3.7 ACCELERATOR RE-USABILITY

Although it was originally intended that the accelerator would be a relatively inexpensive disposable item, it was found in practice that it was possible to re-use the accelerator components extensively. The high gas pressures which occurred in the accelerators were apparently of sufficiently short duration that in most cases no permanent deformation resulted. Exceptions to this were firings 692 and 695, in which pressures up to approximately 750,000 lb/in^2 caused severe bulging near the compression tube and launch tube interface. Severe damage was also caused by gouging in the earlier firings, and in a few of the later firings poor projectile release gave rise to damage at the launch tube entrance.

Accelerators employed in the later stages of the firing program had a hardened bushing at the launch tube entrance. Extensive dressing of the accelerator components was made between firings, including careful honing, and normally the replacement of the bushing at the launch tube entrance.

3.3.8 TWO-GAS ACCELERATOR FIRINGS

Two-gas accelerator firings were intended to explore the possibility of finding a means whereby, for a given primary velocity, base pressures at the secondary projectile may be substantially reduced compared with those experienced in the single-gas accelerator (see also Section 4.1). Only five firings were made to investigate the two-gas concept; these were firings 665, 669, 677, 682 and 686. Largely because of the restricted dump tube

length, the barrel of the light gas gun was employed as the first gas compartment containing the greater mass of gas, as shown in the sketch below.

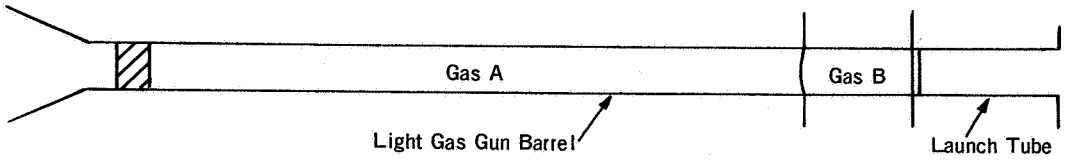

This arrangement was considered to have some possible advantages, which are discussed in Section 4.5. The gas mass ratio M_A/M_B was set equal to 10.0 and the value M_G/M_L was varied between 0.5 and 0.12. Insufficient experience was gained to develop the method, and the technique had to be shelved due to lack of time. The potential value of the two-gas method has therefore not yet been explored.

3.3.9 LIGHT GAS GUN PERFORMANCE

The design of the light gas gun which was used as the primary projectile launcher for the constant area accelerator firings is described in Reference 1. As mentioned in Section 3.2 most firings were made with fixed piston mass, loading pressure and primary projectile mass. Primary projectile velocity is plotted as a function of measured piston velocity in Figure 28; piston velocity versus charge weight is plotted in Figure 29. The gas gun proved to be simple to operate under these conditions, and four firings in a single day were often achieved. Damage to the gun barrel eventually caused the firing program to be terminated slightly prematurely.

SECTION 4

ANALYSIS FROM EXPERIMENTS

4.1 CHOICE OF TWO EXPERIMENTAL APPROACHES

Earlier single-gas accelerator firings employed a value of M_G/M_L which, according to theoretical considerations, minimized the peak base pressure experienced at the secondary projectile. The value used (M_G/M_L = 0.35) meant that the peak base pressure coincided with the arrival of the second or third shock wave at the projectile base, as shown in the representative base pressures sketched in Figure 12. It was felt that this fact may have contributed to early projectile failures, because there might have been a tendency for the projectile to rotate slightly in the launch tube during its initial travel, thereby presenting an inclined rear face to the arrival of the main shock wave.

Reference to Figure 12 shows that for M_G/M_L = 1.0, the peak base pressure is experienced at the arrival of the first shock wave. Figure 10 indicates that for values of M_G/M_L varied between 0.25 and 0.8 approximately there is little change in the magnitude of the peak base pressure. Thus it was decided that a better choice for the value of M_G/M_L would be 0.8, so that maximum base pressure was experienced at the arrival of the first shock wave, while at the same time the magnitude of the peak base pressure was minimized. This choice appeared to be experimentally justified. It was therefore adopted as one of two promising approaches for extending the performance of the accelerator. The above approach is referred to as Approach (a) in Section 3.2.

The alternative approach was the utilization of the two-gas accelerator concept. Although analysis of the two-gas accelerator performance indicated that there might be no performance advantage over the single-gas accelerator, it was found in unsteady gasdynamic computations that a considerable reduction in base pressures would be achieved. It was further thought that it might be possible to eliminate the arrival of shock waves at the projectile base, by evacuating the compartment which normally would contain the second gas. After rupture of the second diaphragm, an escape front will proceed toward the secondary projectile. The projectile may thus experience a relatively gradual pressure rise during its initial travel, rather than a series of shock waves. A limited number of computer runs were made, using the two-gas computer program modified to handle the escape front. Although optimized conditions were not explored, peak base pressures could be reduced below the values plotted for M_A/M_B = 15 in Figure 10.

For the above reasons it was decided to investigate the two-gas accelerator as a means for achieving high velocities. This approach is referred to as Approach (b) in Section 3.2.

4.2 LAUNCH TUBE LENGTH

Initial firings at $M_G/M_L = 0.8$ gave disappointingly low velocity multiplication factors in the neighbourhood of 1.25. Energy loss due to heat transfer from the gas was ruled out as a source of the performance drop, by the fact that similar performance was achieved with hydrogen and helium, although the latter gas gives rise to much higher operating temperatures. The launch tube length, which was approximately half as long as the compression tube in the above firings, was less long than would be suggested by Figure 9. Its length was nevertheless considered adequate, based on the computed base pressure curve shown in Figure 11.

It was realized that an error in computing the position of the second shock wave could occur due to uncertainty in such factors as the gas co-volume, and contamination; and that experimental lateness of this shock wave would lead to performance degradation. Accordingly, it was decided to increase the launch tube length to nine inches, or approximately equal to the compression tube length (8.4 inches). This improved the velocity multiplication factor considerably and it was inferred that the above diagnosis was correct.

4.3 PROJECTILE DYNAMICS

The most important problem which has prevented development of the accelerator to high velocities has been the lack of understanding of the mechanics of the secondary projectile failure. Experimental evidence has shown clearly that high pressure alone is not the principal factor which governs failure. The solution to the problem lies in the understanding of the complex unsteady wave motions which are set up in the projectile (and also in the gas and the launch tube walls). It is shown below that, if projectiles are sufficiently long, failure may occur in the form of spall-like tensile fractures, and this has been observed experimentally with plastic projectiles. On the other hand, it appears that very short projectiles can lead to serious problems. Experimental firings with 0.025 calibre long aluminum disks have failed consistently for base pressures as low as 150,000 lb/in^2, while a 0.1 calibre projectile has survived a base pressure in excess of 700,000 lb/in^2 and was launched in excellent condition. A discussion of possible failure modes of long and short projectiles is given in the succeeding subsections.

4.3.1 FAILURE OF LONG PROJECTILE

A one-dimensional view of the wave propagation of a projectile accelerating under the influence of a gas shock wave arriving at its base leads to the following simplified wave diagram.

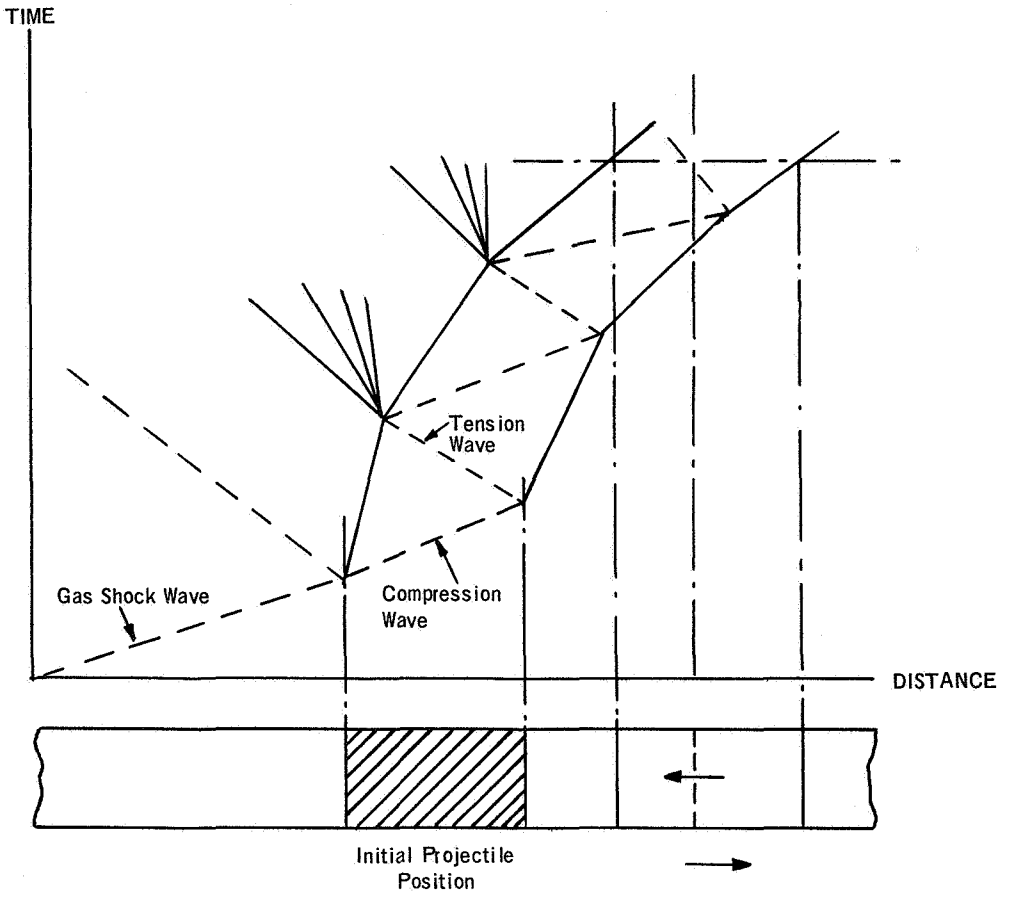

The initial compressive wave in the projectile material reflects from the front face as a tensile wave of equal and opposite magnitude, and brings the stress in the projectile to zero if no external influences are present in the gas. If, however, a strong forward propagating rarefaction is present in the gas, this will react with the wave system in the projectile to produce tensile stresses. Such a forward propagating rarefaction would be produced by the decelerating primary projectile*. By shortening the projectile, and employing a material with high wave speed, it is possible to reduce the transit time and hence limit the magnitude of the tensile stresses.

* Tensile failure of the primary projectile is observed on most firings. In this case the required backward propagating rarefaction wave is provided by the accelerating projectile.

Computer studies reported in Reference 5 showed that the launch tube wall effects modify this picture considerably, and for the long projectiles (over one calibre) considered there was a tendency to reduce tensile stresses. It is not known what the wall effects are for short projectiles.

4.3.2 FAILURE OF SHORT PROJECTILES

A number of possible modes of failure of the short disk-like projectiles has been considered during the present investigation. The most obvious is the possibility that the projectile will become misaligned during its travel, which might cause it to impinge on the accelerator wall upon the arrival of a strong shock wave. This possibility led to the adoption of an accelerator operating cycle which concentrated peak pressure at the start of motion.

A second possibility is that the mechanics of the projectile release can lead to failure. Initially the projectile must be supported against the accelerator gas loading pressure, which usually is in the range 600 to 1100 lb/in^2. Experimental evidence indicated that the release of the projectile was a source of difficulty and a number of firings were made in an attempt to overcome this problem. These firings are described in Section 3.3.3.

The least understood aspect of the failure of the short projectiles is the experimental fact that, as the disk length is reduced, so also is the peak base pressure which it can withstand. Possible areas which have been considered are:

(a) Effect of initial surface finish

(b) Effect of initial static deflection under accelerator loading pressure

(c) Effect of dynamic flexing due to the wave system in the projectile

Possibility (a) received close attention when it was realized that minor scratches or imperfections were much more serious in the case of the very short 0.025 L/D projectiles. Care in preserving surface finish did not result in any experimental improvement. Possibility (b) arises because of the greatly increased tendency of a diaphragm to deflect as its thickness is reduced. The deflection increases fourfold for the 0.025 L/D projectile as compared with the 0.050 L/D projectile, even though the loading pressure is halved. This deflection will affect the initial passage of the first

compression wave through the projectile. As indicated in the sketch blow, the gas dynamic shock wave will arrive at the outer circumference first and will compress this material and start it in motion.

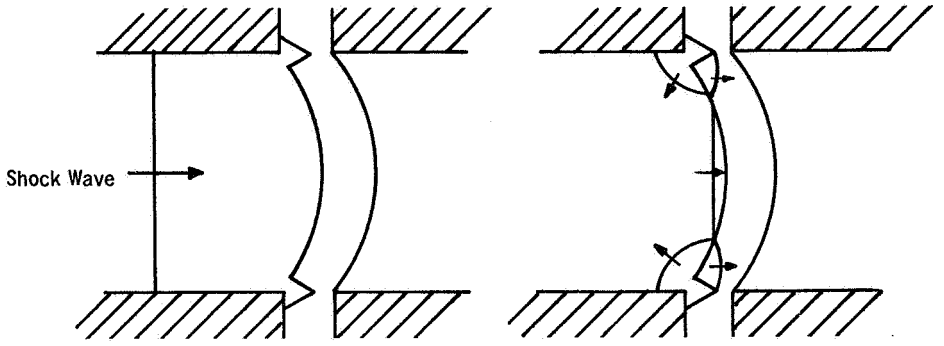

This would have the effect of accelerating the outer material in advance of the centre of the projectile, and may help to explain the reason why, in many firings, the projectile has been observed to be dished "the wrong way" after launch; that is, it is concave on the front face. In the case of the 0.025 L/D projectile, the situation is so extreme that the compression wave can pass through the projectile at the circumference and reflect from the forward face, before the gas shock wave is felt at the centre of the projectile.

Possibility (c) arises from the unsteady wave system existing in the projectile during the initial acceleration, as indicated in the sketch below.

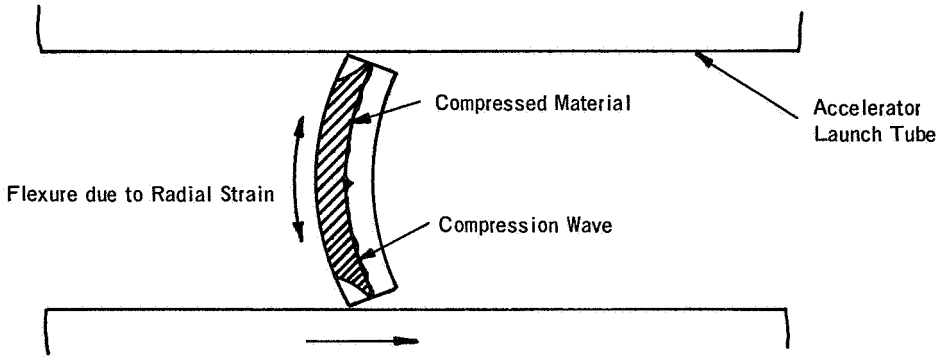

Passage of the compression waves may cause the projectile to undergo flexing oscillations. The situation will be very complicated, especially if wall effects are present at the circumference. If such flexing occurs this may also provide an explanation for the reverse dishing which is observed. A

computer program was written to simulate the flexing mode, in which the stress propagation equations were expressed in a finite-difference form. The object was to gain some insight into possible failure-producing mechanisms. Unfortunately some stability difficulties were encountered and the program was shelved due to lack of time.

4.4 ELIMINATION OF ACCELERATOR GOUGING

In earlier firings a form of gouging damage was often experienced at the entrance to the accelerator at the diaphragm position, apparently caused by the entry of the primary projectile. In some firings range pressure was left fairly high (2400 microns or more), in an attempt to introduce cushioning air into the barrel, which was evacuated to range pressure. In spite of this, some gouging damage persisted. The primary case of the gouging was not clear, because in some cases it appeared that severe pressure between the primary projectile and the accelerator wall had pushed accelerator material forward, whereas in other cases the 'gouging' took the form of pitting or gas wash. It was strongly suspected that heat, generated in the cushion of air ahead of the primary projectile, might have been a major contributory factor. It was reasoned that hydrogen would offer a chance of overcoming this difficulty, since for a given internal energy hydrogen is very much cooler than air. Calculations indicated that hydrogen at a pressure 75 mm would provide an effective gas cushion without slowing the primary projectile unduly. This measure was adopted, and was found to eliminate this form of gouging.

4.5 GAS GUN BARREL AS COMPRESSION TUBE

In all two-gas accelerator firings, the barrel of the light gas gun was utilized as the first gas compartment, containing the larger mass of gas. Besides convenience, the method was thought to have the following advantages. First, there is less chance of possible leakage of the loading gas from the accelerator after loading but prior to firing. Third and perhaps most important, the compression in the gas gun barrel heats the gas to very high temperatures and as a result it may be possible to reduce the severity of the shock waves which are transmitted to the projectile base. Disadvantages of this method include the fact that the actual pressure history on the base of the projectile is difficult to predict, and as a result an adequate launch tube length is hard to choose.

Computer runs were made with a modified program developed to handle the acceleration of the primary projectile in the gun barrel. These were used to investigate the compression of helium and hydrogen gas and

determine the point at which the secondary projectile or diaphragm releases. These runs indicated that, using typical masses of hydrogen gas, release would occur when the primary projectile was within one foot of the projectile or diaphragm. In actual practice the separation will be different, since uniform acceleration of the projectile was assumed, however the method appeared sufficiently promising to form the basis of a number of exploratory firings.

SECTION 5

DISCUSSIONS AND CONCLUSIONS

5.1 ACCELERATOR PERFORMANCE

Best performances, in terms of secondary projectile velocity and velocity multiplication factor, were achieved by the single-gas accelerator employing a projectile mass ratio M_P/M_L of 18.0; and a ratio of gas mass to secondary projectile mass, M_G/M_L, equal to 0.8. Secondary velocities of over 30,000 feet/second were achieved from primary velocities slightly under 20,000 feet/second.

Perhaps the most encouraging aspect of the accelerator performance has been the fact that the velocity multiplication factors have shown little tendency to decrease over the range of primary velocities which was investigated. This agrees with the accelerator theory and indicates that energy losses have not been restrictive. At the highest primary velocities used, the secondary velocity was only from five to fifteen percent below the theoretically predicted values. It is clear that the accelerator concept is capable of much higher performance with higher primary projectile velocities.

For reasons outlined earlier, disk-like metal secondary projectiles (mostly aluminum) were employed to achieve the desired high values of the ratio M_P/M_L, which is the major parameter governing accelerator performance. The attainment of higher performance was restricted by the anomalous failure characteristics of the projectiles under the high base pressures applied in the accelerator. These characteristics are further discussed below. In particular it was not possible to achieve higher multiplication factors by increasing M_P/M_L (i.e. reducing M_L); because the thinner disks which were entailed exhibited greater fragility, even though base pressures were reduced in proportion to the projectile mass.

Increased performance capability probably would have resulted if longer accelerators had been employed, thereby reducing base pressure levels. This would, however, have entailed further lengthening of the dump tank, which was undesirable due to space limitations.

Theoretical studies of the two-gas accelerator suggested that this concept offered a means of greatly reducing base pressures compared with the single-gas accelerator. Unfortunately only a few two-gas accelerator firings were made, and it was not possible to develop the technique. The firing program concentrated on the single-gas accelerator because it was

felt that it was undesirable to divide effort on a program having such a relatively short time scale (four months). It is nevertheless felt that the two-gas concept is extremely promising and may eventually be the means whereby the highest accelerator performances are achieved.

5.2 PROJECTILE FAILURE

For the single-gas accelerator configurations which were examined in this study, an upper limit was placed on performance by the base pressure capabilities of the disk-like secondary projectiles. It was found that there was a strong and unexplained dependency of the peak base pressures at which failure occurred, on the length to diameter ratios of the projectile; thicker projectiles being able to withstand higher pressures. This dependency was not attributable to variations in material, manufacturing methods or surface finish. Possible causes were the initial static deflection of the projectile as a diaphragm, due to the loading gas pressure; and the effect of dynamic flexing due to the unsteady wave propagation system set up in the projectile by the arrival of shock waves. The dynamic flexing mode is such that at maximum amplitude the projectile would assume a saucer shape with the concave surface forward. Saucer shaped intact projectiles were often observed experimentally, normally with the concave surface to the front.

Insufficient time was available to ascertain the degree to which performance may be enhanced by the use of lighter metal alloys than aluminum, such as magnesium and magnesium-lithium alloys. The latter alloy would permit an increase in projectile L/D ratio to 0.1 from 0.05 for aluminum, in the accelerator configurations studied.

5.3 OVERALL CONCLUSIONS

The accelerator concept appears to be entirely valid, in that experimental tests gave good agreement with theory, and indicated that energy losses will not restrict the development of the accelerator to a very high performance. Extrapolation of the experimental results indicates that velocities of 45,000 feet/second will be achievable at the top end of the light gas gun performance. However, it appears to be possible to develop the accelerator configuration to produce higher values of velocity multiplication, so that the accelerator has a much higher velocity potential.

Accelerator performance was limited by the anomalous failure characteristics of the disk-like projectiles. Further accelerator development should place a strong emphasis on the understanding of unsteady stress

wave propagations in the projectile, whether or not disk-like projectiles continue to be employed. Such a study must be tied not only to the gas shock and rarefaction processes, but also to stress waves generated at the launch tube wall.

SECTION 6

RECOMMENDATIONS

The experimental program has demonstrated that the constant area accelerator has an extremely promising potential for development to much higher velocities. Difficulties in the program were mainly associated with the failure characteristics of the very short disk-like projectiles.

The experimental program was subject to the restriction of a short dump tank, which limited the accelerator length. This restriction was felt to be unnecessarily severe. In terms of overall velocity capability, for example, it might well be more advantageous to increase the accelerator length by, say, one foot at the expense of a one foot decrease in the gun barrel length.

Based on the above, it is recommended that further development of the accelerator should proceed as follows:

An accelerator configuration should be sought in which increased L/D metal projectiles may be employed; not only because of the above failure characteristics, but also because disk-like projectiles are not an attractive proposition for development as a carrier, holding a third, smaller projectile.

The experimental development should be supported by a theoretical study of stress wave propagations in the projectile. This study would be aimed at gaining an increased understanding of the factors governing projectile damage, so that such damage may be avoided.

The accelerator should be developed without restricting its length due to space limitations. The latter may be considered when the best accelerator formula for high performance has been determined.

REFERENCES

1	Cowan, P.L.	Development of a Micrometeoroid Simulation Device, Volume 1. Computing Devices of Canada, Report 7456/R1, October 1967.
2	Murphy, J.R.B. Badhwar, L.K. Lavoie, G.A.	Interior Ballistic Calculation Systems for Light Gas Guns and Conventional Guns. AGARD Specialists Meeting on "Fluid Dynamic Aspects of Ballistics" Mulhouse, France 1966.
3	Badhwar, L.K.	Hydrodynamic Simulation of Hypervelocity Impact. Computing Devices of Canada 3471/PR2. August 1966.
4	Moore, E.T. et al	Recent Developments in the Use of Chemical Explosives for Hypervelocity Test Devices. Fifth Hypervelocity Techniques Symposium 16-17 March 1967.
5	Watson, J.D., and Godfrey, C.S.	An Investigation of Projectile Integrity Using Computer Techniques. Fifth Hypervelocity Techniques Symposium 16-17 March 1967.

APPENDIX A

SIMPLIFIED ANALYSIS — ONE GAS CASE

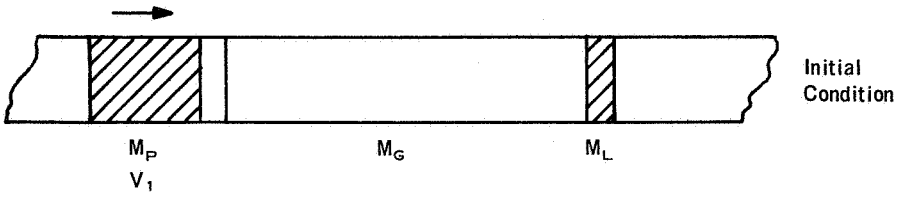

If no external forces act on the system, then the final conditions may be related to initial conditions by simple equations of conservation of momentum and energy. If it is assumed that the gas density is uniform when the final conditions are achieved, then the gas momentum and kinetic energy may be expressed in terms of the projectile velocities as follows:

$$\text{gas momentum} = M_G \frac{V_2 + V_L}{2}$$

$$\text{gas kinetic energy} = \frac{M_G}{2} \frac{(V_2^2 + V_L V_2 + V_L^2)}{3}$$

where M_G = gas mass

V_2 = final primary projectile velocity

V_L = final secondary projectile velocity (launch velocity).

The system momentum and energy conservation equations may then be written:

$$\text{momentum: } M_P V_1 = M_P V_2 + M_G \frac{V_2 + V_L}{2} + M_L V_L$$

$$\text{energy: } M_P V_1^2 = M_P V_2^2 + K M_G \frac{(V_2^2 + V_L V_2 + V_L^2)}{3} + M_L V_L^2$$

where M_P = mass of primary projectile

M_L = mass of secondary projectile

K = factor expressing loss of kinetic energy to gas internal energy or heat losses.

V_L may then be expressed as follows:

$$\frac{V_L}{V_1} = \frac{-b \pm \sqrt{b^2 - 4ac}}{2a}$$

where

$$a = B^2\left(\frac{M_P}{M_G} + \frac{K}{3}\right) + \frac{M_L}{M_G} + \frac{K}{3}(1 - B)$$

$$b = \frac{KA}{3} - 2AB\left(\frac{M_P}{M_G} + \frac{K}{3}\right)$$

$$c = A^2\left(\frac{M_P}{M_G} + \frac{K}{3}\right) - \frac{M_P}{M_G}$$

$$A = \frac{2M_P}{2M_P + M_G} \qquad B = \frac{2M_L + M_G}{2M_P + M_G}$$

APPENDIX B

SIMPLIFIED ANALYSIS — TWO GAS CASE

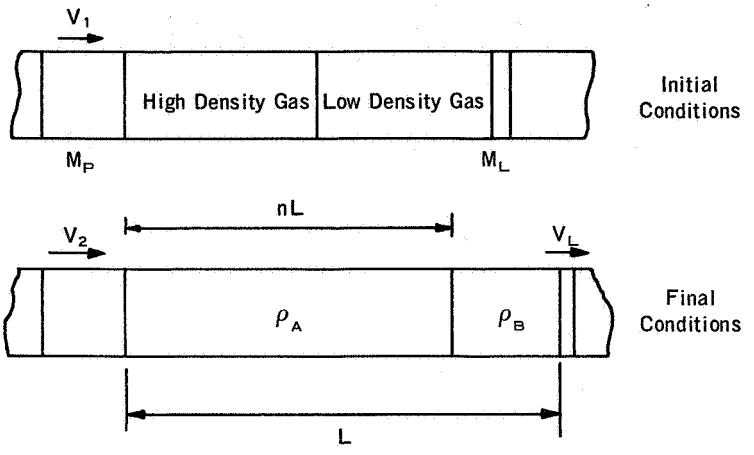

If no external forces act on the system, then the final conditions may be related to initial conditions by simple equations of conservation of momentum and energy. If it is assumed that the gas density in each compartment is uniform when the final conditions are reached, then the gas momentum and kinetic energy may be expressed as follows:

gas momentum:

$$\left\{ \begin{array}{l} V_2 \left[\rho_n AL\, n \left(1 - \frac{n}{2}\right) + \rho_B\, AL \left(\frac{1}{2} - n + \frac{n^2}{2}\right) \right] \\ + V_L \left[\rho_n AL\, \frac{n^2}{2} + \rho_B AL \left(\frac{1 - n^2}{2}\right) \right] \end{array} \right.$$

gas kinetic energy:

$$\left\{ \begin{array}{l} V_2^2 \left[\rho_A \frac{AL}{2} \left(n - n^2 + \frac{n^3}{3}\right) + \rho_B \frac{AL}{2} \left(n^2 - n + \frac{1 - n^3}{3}\right) \right] \\ + V_L^2 \left[\rho_A \frac{AL}{2} \left(\frac{n^3}{3}\right) + \rho_B \frac{AL}{2} \left(\frac{1 - n^3}{3}\right) \right] \\ + V_L V_2 \left[\rho_A \frac{AL}{2} \left(n^2 - \frac{2n^3}{3}\right) + \rho_B \frac{AL}{2} \left(1 - n^2 - 2\,\frac{(1 - n^3)}{3}\right) \right] \end{array} \right.$$

$$= X. \frac{V_2^2}{2} + Y. \frac{V_L^2}{2} + Z. \frac{V_L V_2}{2} \quad \text{say}$$

The system momentum and energy conservations may then be written:

momentum: $$M_p V_1 = M_p V_2 + V_2\left[\rho_n A L_n \left(1 - \frac{n}{2}\right) + \rho_B A L\left(\frac{1}{2} - n + \frac{n_2^2}{2}\right)\right]$$

$$+V_L\left[\rho_A A L \frac{n^2}{2} + \rho_B A L\left(\frac{1 - n^2}{2}\right)\right] + M_L V_L$$

energy: $$M_p V_1^2 = M_p V_2^2 + K\left(X.\frac{V_2^2}{2} + Y.\frac{V_L^2}{2} + Z.\frac{V_L V_2}{2}\right) + M_L V_L^2$$

In the above:

ρ_A = density in compartment A

ρ_B = density in compartment B

n = position of interface as fraction of L

L = length of gas column

V_1 = initial primary projectile velocity

V_2 = final primary projectile velocity

V_L = final secondary projectile velocity

A = accelerator cross section

M_p = primary projectile mass

M_L = secondary projectile mass

K = factor expressing loss of kinetic energy to gas internal energy or heat losses

The above relationships are then solved to give the velocity multiplication factor V_L/V_1.

Accelerator Geometry		Firing Number	Date	Primary* Velocity ft/sec(V_l)	Primary Condition (X-Ray)	Accelerator Gas		Secondary Projectile		Secondary Condition (X-Ray)	Secondary Velocity ft/sec(V_L)	Accelerator Condition	Remarks	
Comp Tube	Launch Tube					Gas	M_G/M_L	Mat'l	Wt Gm					
5.5 in.	4.75 in.	616	4 Nov 66	≈ 15,000	Good	He	.125	Nylon	0.8	Broken Up	18,400	Good		
5.5	4.75	619	9 Nov	≈ 15,000	Good	He	.11	Zelux	0.9	Broken Up	N.R.	Good		
5.5	4.75	625	18 Nov	≈ 16,050	Good	He	1.0	Al	0.1	---------	N.R.	Slight Gouge		
4.5	4.75	628	24 Nov	≈ 17,000	N.V.	He	0.8	Al	0.1	N.V.	Not Confirmed	Good	X-Rays Poor	
5.5	5.25	630	2 Dec	≈ 17,000	N.V.	He	0.8	Al	0.1	N.V.	Not Confirmed	Slight Gouge	X-Rays Poor	
4.5	5.25	632	5 Dec	≈ 16,000	Good	He	0.35	Al	0.22	N.V.	Not Confirmed	Very Good	X-Rays Poor	
4.5	5 25	634	13 Dec	11,800	Good	He	0.35	Al	0.22	Slight Bend	18,700	Very Good	Velocity from X-rays	
4.5	5.25	635	14 Dec	14,750	Broken	He	0.35	Al	0.22	Very Good	22,300	Very Good		
4.5	5.25	636	14 Dec	16,200	Broken	He	0.35	Al	0.22	Very Good	23,600	Good		
4.5	5.25	637	16 Dec	17,750	Broken	He	0.35	Al	0.22	Very Good	25,900	Good		
4.5	5.25	638	16 Dec	19,400	Disinte-grated	He	0.35	Al	0.22	Broken	23,600	Gouge		
5.25	5.25	640	21 Dec	18,900	Broken	He	0.50	Al	0.22	Good	25,000 - 30,000	Good	One X-Ray Only	
5.25	5.25	642	21 Dec	17,700	Broken	He	0.40	Al	0.14	N.V.	N.R.	Deep Gouge		
4.5	5.25	643	23 Dec	17,600	Good	He	0.27	Al	0.13	Particle Only	N.R.	Gouge		
5.25	5.25	645	23 Dec	18,800	Good	He	0.29	Al	0.22	Broken	21,000	Gouge		
5.25	5.25	646	28 Dec	17,900	Good	He	0.47	Al	0.20	Particles	N.R.	Deep Gouge		
4.75	5.25	647	28 Dec	17,600	Broken Up	He	0.42	Al	0.22	Good	25,000	Slight Gouge		
8.4	4.25	648	30 Dec	18,700	Completely Disintegrated	He	0.40	Al	0.22	Slight Bend	21,000	Very Bad Gouge		
8.4	4.25	649	30 Dec	18,800	Broken	He	0.40	Al	0.22	Deformed	22,200	Good		
				*Inferred from Piston Velocity										

Table 1.

FOLDOUT FRAME 1

Table 1. Summary of Accelerator Development Firings (Sheet 1 of 4)

FOLDOUT FRAME 2

Accelerator Geometry		Firing		Primary*	Primary	Accelerator Gas		Secondary Projectile		Secondary	Secondary	Accelerator		
Comp Tube	Launch Tube	Number	Date	Velocity ft/sec(V_1)	Condition (X-Ray)	Gas	M_G/M_L	Mat'l	Wt Gm	Condition (X-Ray)	Velocity ft/sec(V_L)	Condition	Remarks	
8.4 in.	4.25 in.	650	6 Jan 67	18,800	Broken Up	He	0.84	Al	0.22	Excellent	24,000	Excellent		
4.5	5.25	651	6 Jan	17,800	Broken Up	He	0.42	Al	0.22	N.V.	------	Excellent		
8.4	4.25	652	6 Jan	18,800	Deformed	He	0.84	Al	0.22	Excellent	23,500	Bad Gouge		
8.4	4.25	653	13 Jan	18,750	Good	He	0.84	Al	0.22	Excellent	23,700	Excellent	H_2 in LGG Barrel 75mm	
8.4	4.25	654	13 Jan	18,800	Good	He	0.26	Al	0.22	Damaged	26,000	Excellent		
8.4	4.25	655	13 Jan	18,900	Very Good	He	0.84	Al	0.11	N.V.	------	Excellent		
8.4	4.25	656	20 Jan	18,900	Good	H_2	0.87	Al	0.11	N.V.	------	Excellent		
8.4	4.00	657	20 Jan	18,800	Damaged	H_2	0.26	Al	0.22	Intact, Damaged	25,400	Excellent		
8.4	4.00	658	23 Jan	18,750	Good	H_2	0.8	Al	0.22	Very Good	23,000	Excellent		
4.5	5.25	659	27 Jan	18,050	Good	He	0.36	Al	0.22	Broken	------	Launch Tube Pitted		
4.5	5.25	660	27 Jan	18,700	Good	He	0.8	Al	0.22	Broken	------	Launch Tube Pitted		
8.4	4.00	661	27 Jan	18,900	Good	He	0.15	Al	0.22	Broken	------	Very Good		
4.4	5.25	663	3 Feb	18,700	Deformed	He	0.33	Al	0.22	Broken Up	------	Good		
LGG Barrel	4.25	664	3 Feb	17,700	N.V.	H_2	0.36	Al	0.22	N.V.	------	Excellent		
LGG Barrel	5.25	665	3 Feb	17,900	Excellent	H_2	0.5	Al	0.22	Intact	11,000	Excellent	Two-Gas Firing	
8.4	9.0	668	10 Feb	18,600	Deformed	He	0.84	Al	0.22	Broken	20,000	Launch Tube Damaged		
LGG Barrel	13.0	669	10 Feb	17,800	N.V.	H_2	0.5	Al	0.22	Intact	23,700 ?	Excellent	Two-Gas Firing	
LGG Barrel	13.0	670	10 Feb	17,850	N.V.	H_2	0.36	Al	0.22	N.V.	------	Excellent		
8.4	9.0	676	17 Feb	18,600	Good	He	0.84	Al	0.22	Good	29,000-31,000	Launch Tube Damaged		
LGG Barrel	13.0	677	17 Feb	17,600	N.V.	H_2	0.5	Al	0.22	Good	12,000	Slight Damage	Two-Gas Firing	
8.4	4.25	678	17 Feb	18,800	Excellent	H_2	0.84	Al	0.12	Broken Up	------	Excellent		

Table 1.

Table 1. Summary of Accelerator Development Firings (Sheet 2 of 4)

Accelerator Geometry		Firing Number	Date	Primary Velocity ft/sec(V_1)	Primary Condition (X-ray)	Accelerator Gas		Secondary Projectile		Secondary Condition (X-ray)	Secondary Velocity ft/sec (V_L)	Accelerator Condition	REMARKS	
Comp. Tube	Launch Tube					Gas	M_G/M_L	Mat'l	Wt. Gm.					
8.4inches	9.0 inches	681	24 Feb	18,800	Deformed	He	0.84	Al	0.22	Excellent	28,000	Launch Tube Damaged		
L.G.G. Barrel	13.0	682	24 Feb	17,800	Excellent	H_2	0.25	Al	0.22	Good	13,000	Excellent	Two-Gas Firing	
8.4	9.0	683	24 Feb	19,400	Good	He	0.84	Al	0.22	Broken	22,500	Launch Tube Damaged		
8.4	4.5	684	24 Feb	19,450	Good	He	0.36	Al	0.22	Broken	27,000	Launch Tube Damaged		
L.G.G. Barrel	13.0	686	27 Feb	17,900	Good	H_2	0.12	Al	0.22	Broken	18,000	Excellent	Two-Gas Firing	
8.4	9.0	687	27 Feb	19,400	Good	He	0.84	Al	0.22	Small particles-Mylar	17,000 55,000	Launch Tube Damaged		
8.4	9.0	692	3 Mar	19,350	Deformed	He	0.7	Al	0.45	Good	N R.	Comp. Tube Expanded		
8.4	9.0	693	3 Mar	19,400	Deformed	He	0.84	Al	0.22	Broken	23,500	Launch Tube Damaged	Release Test	
8.4	9.0	694	6 Mar	18,900	Deformed	A	0.8	Al	0.22	Broken	--	Launch Tube Damaged	Release Test	
8.4	9.0	695	6 Mar	19,400	--	He	0.84	Al	0.36	Good	23,800	Comp. Tube Expanded		
8.4	9.0	700	14 Mar	19,450	Very Good	A	0.84	Al	0.22	N.V.		Good	Release Test	
8.4	9.0	701	14 Mar	19,350	Good	He	0.84	Al	0.22	Broken	~20,000	Launch Tube Damaged	Release Test	
8.4	9.0	704	14 Mar	19,400	Good	He	0.84	Al	0.22	Good	27,900	Good	Release Test	
8.4	9.0	706	17 Mar	19,400	Good	He	0.84	Mg.	0.22	Very Good	28,100	Good		
8.4	9.0	707	15 Mar	19,800	Good	He	0.84	Al	0.22	Intact Bent	28,000	Good		
8.4	9.0	708	17 Mar	19,700	Good	He	0.84	Mg.	0.22	Broken in Half	27,800	Good		
8.4	9.0	709	17 Mar	19,850	Good	He	0.84	Al	0.22	Broken	--	Launch Tube Damaged		
8.4	9.0	710	20 Mar	19,500	Deformed	He	0.84	Mg.	0.22	Broken	--	Good		
8.4	9.0	715	23 Mar	19,250	--	He	0.84	Mg.	0.22	Broken	--	Good	Release Test	
8.4	9.0	716	23 Mar	19,200	Deformed	He	0.84	Mg.	0.22	N.V. due Velocity	31,500 33,000	Good	Release Test	
8.4	9.0	717	27 Mar	19,200	Damaged	He	0.84	Mg.	0.22	Broken	--	Launch Tube Damaged	Release Test	

Table 1.

Table 1. Summary of Accelerator Development Firings (Sheet 3 of 4)

Accelerator Geometry		Firing Number	Date	Primary* Velocity ft/sec(V_1)	Primary Condition (X-Ray)	Accelerator Gas		Secondary Projectile		Secondary Condition (X-Ray)	Secondary Velocity ft/sec(V_L)	Accelerator Condition	Remarks	
Comp Tube	Launch Tube					Gas	M_G/M_L	Mat'l	Wt Gm					
8.4 in.	9.0 in.	720	31 Mar 67	19,200	Badly Damaged	He	0.84	Li/Mg	0.22	Good	28,000	Launch Tube Damaged	LGG Barrel Damaged (720–721)	
8.4	9.0	721	31 Mar	19,700	Broken	He	0.84	Li/Mg	0.22	Good, Bent	20,000	Good		
8.4	9.0	723	3 Apr	19,900	N.V	He	0.84	Li/Mg	0.22	Broken	------	Good		

Table 1.

Table 1. Summary of Accelerator Development Firings (Sheet 4 of 4)

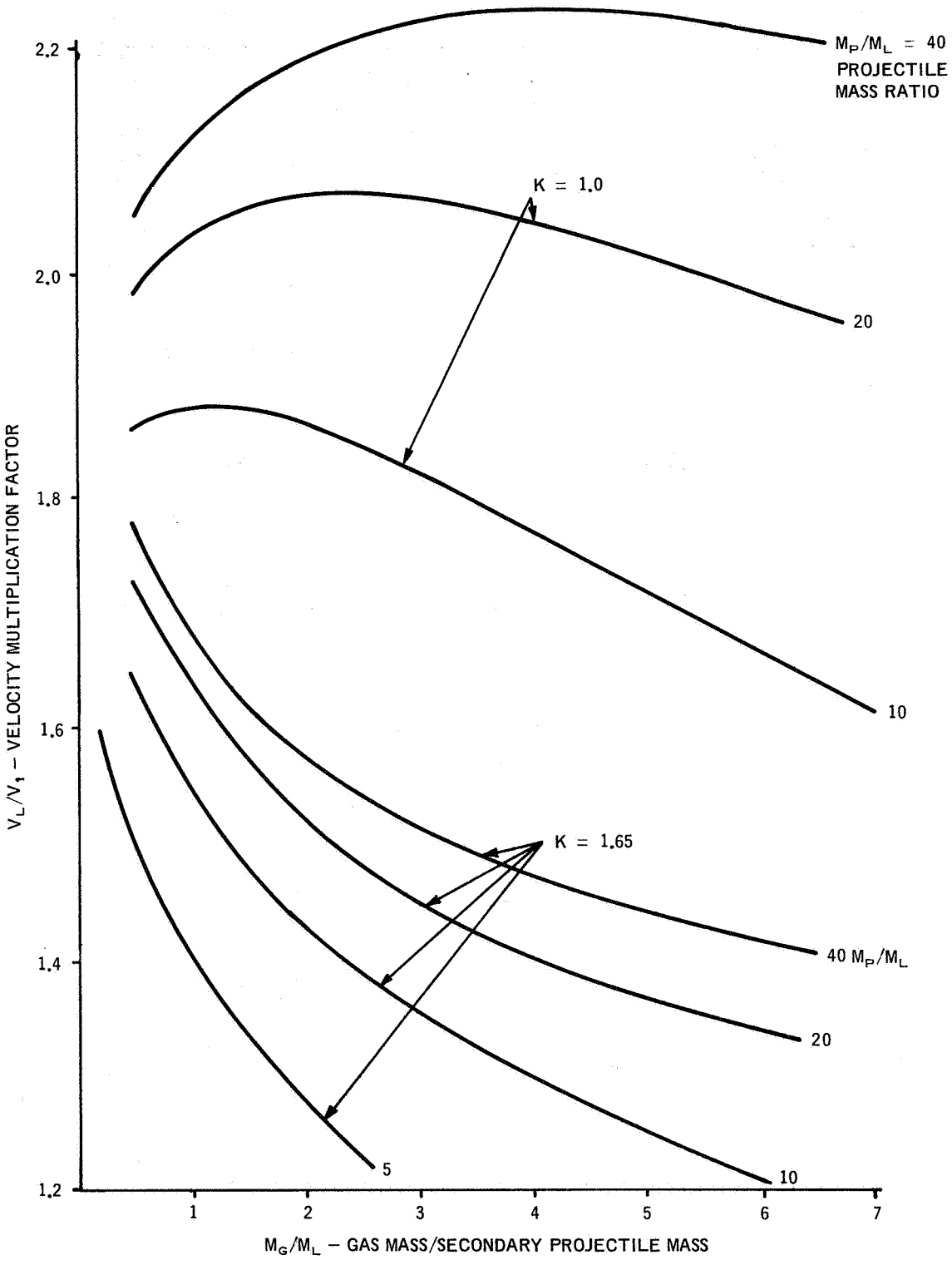

Figure 1. Typical Multiplication Factors from Simplified Analysis - Single-Gas Accelerator

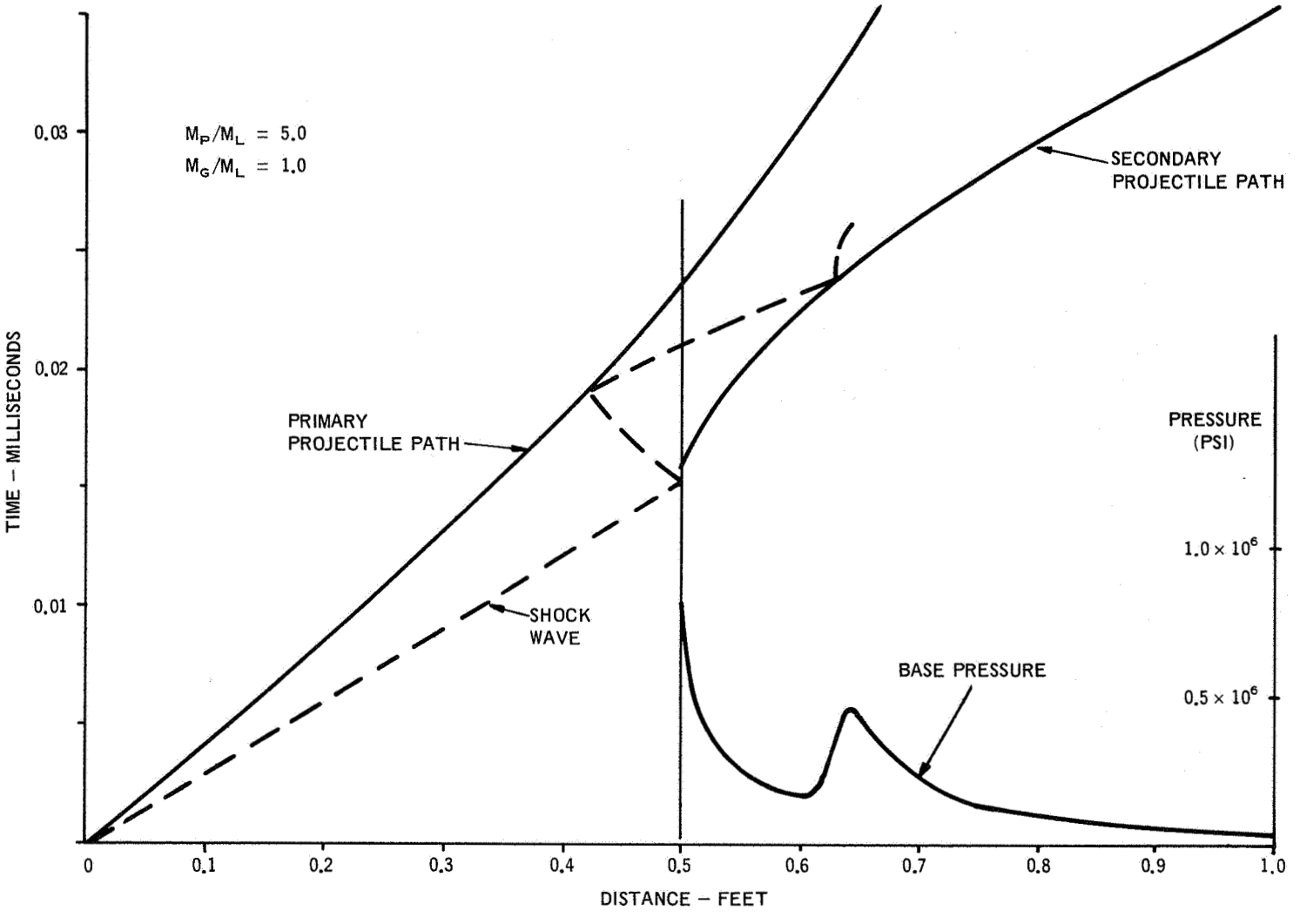

Figure 2. Computed Distance/Time Diagram for Helium

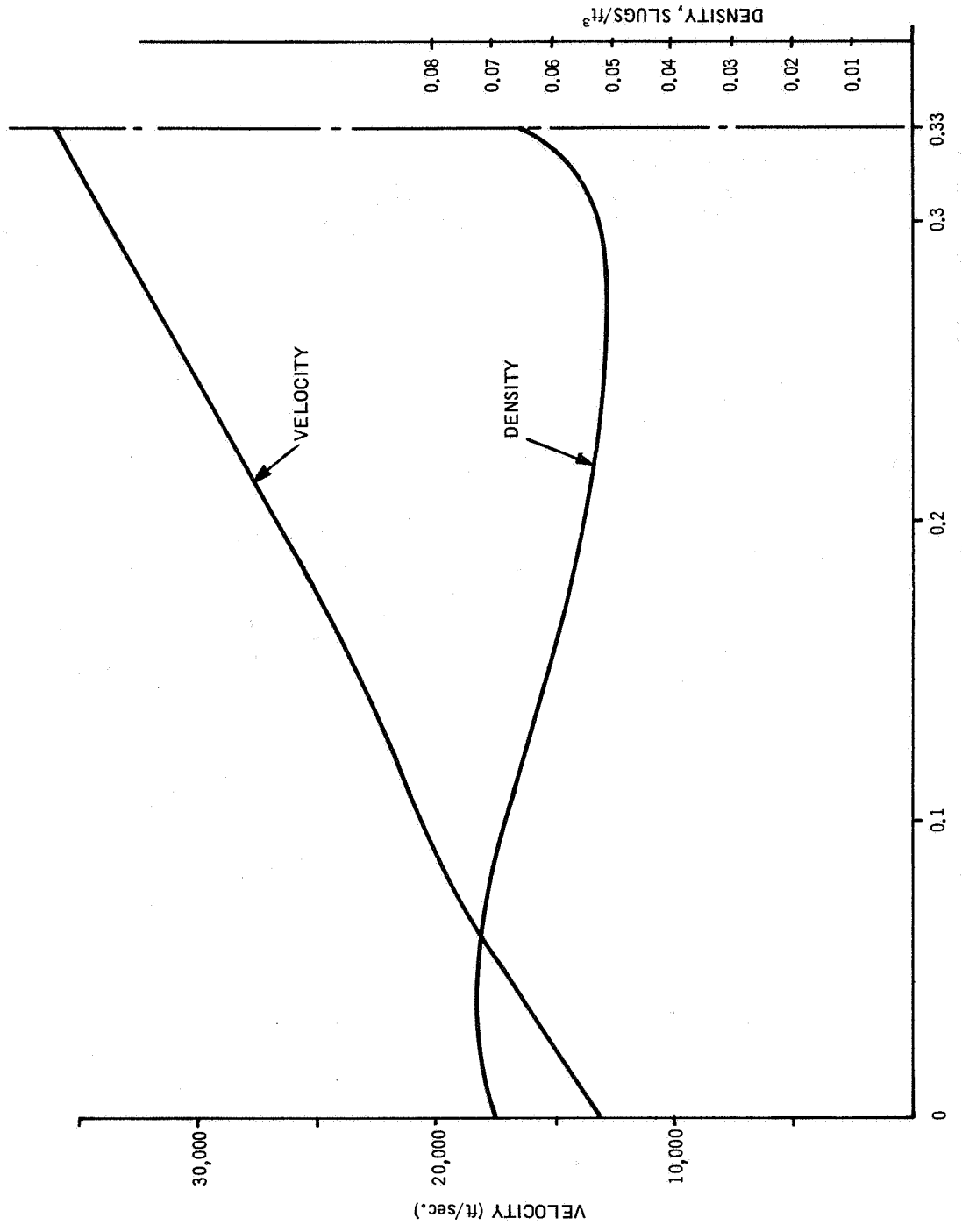

Figure 3. Computed Velocity and Density Distributions at Late Time-Helium

Figure 3.

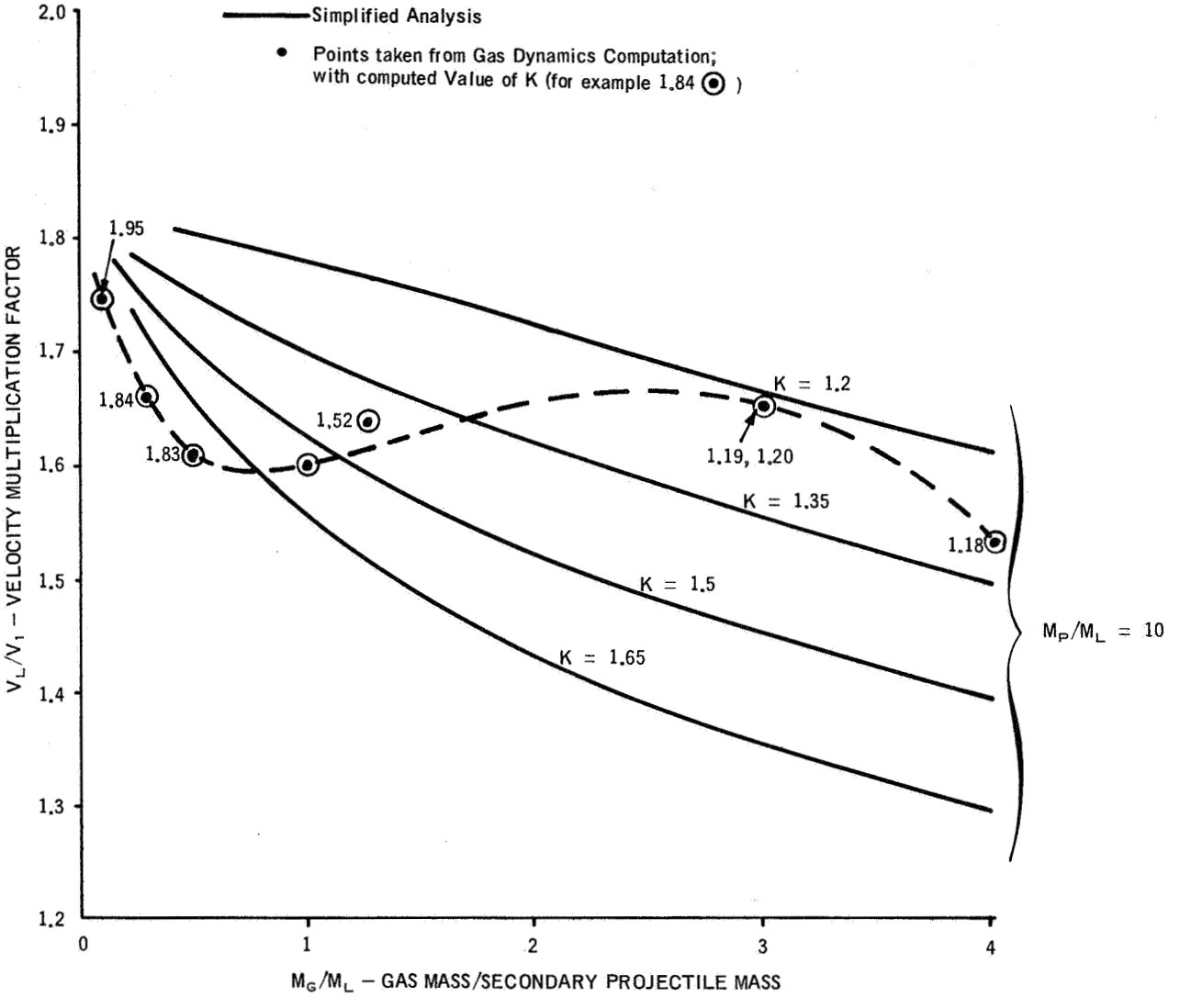

Figure 4. Comparison of Gasdynamic Computations with Simplified Analysis at $M_P/M_L = 10$

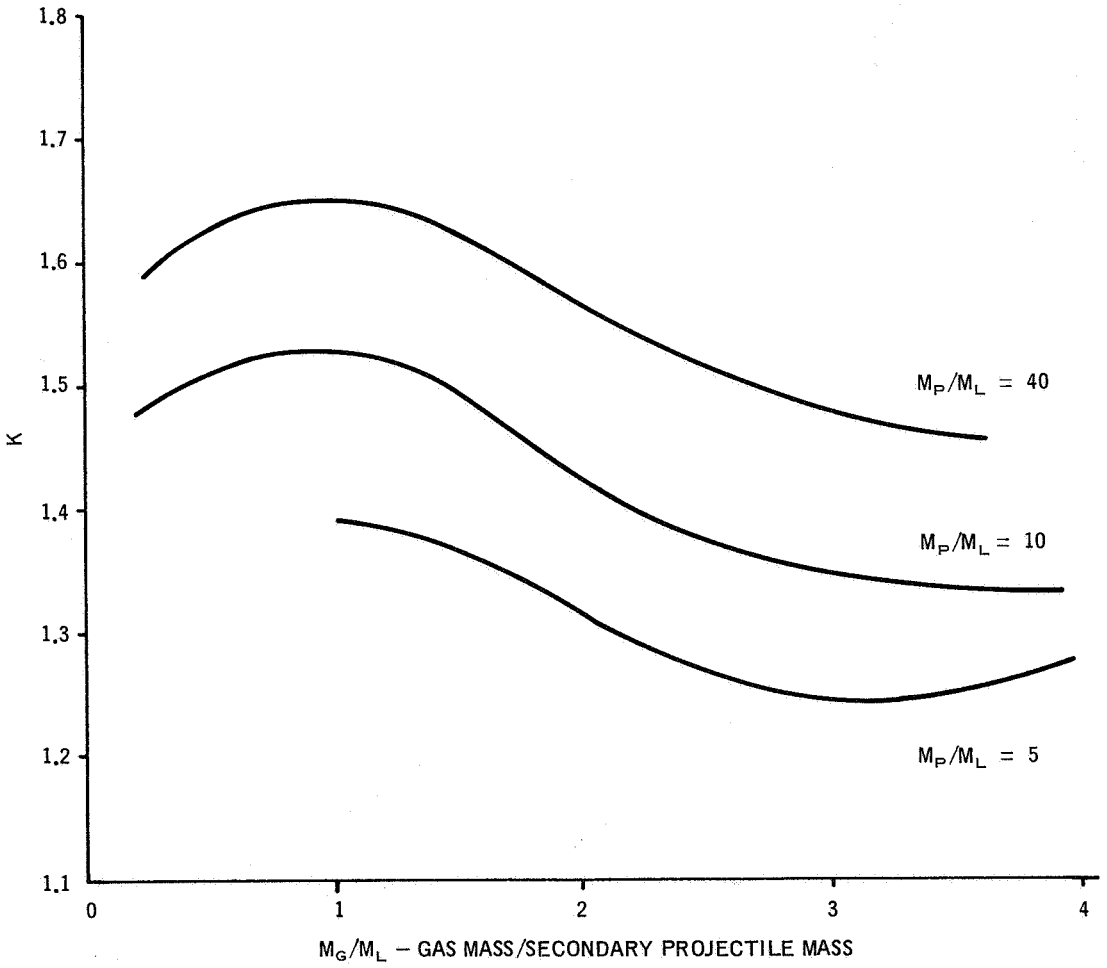

Figure 5. Variation of Energy Loss Factor 'K' with M_G/M_L - Criterion (a)

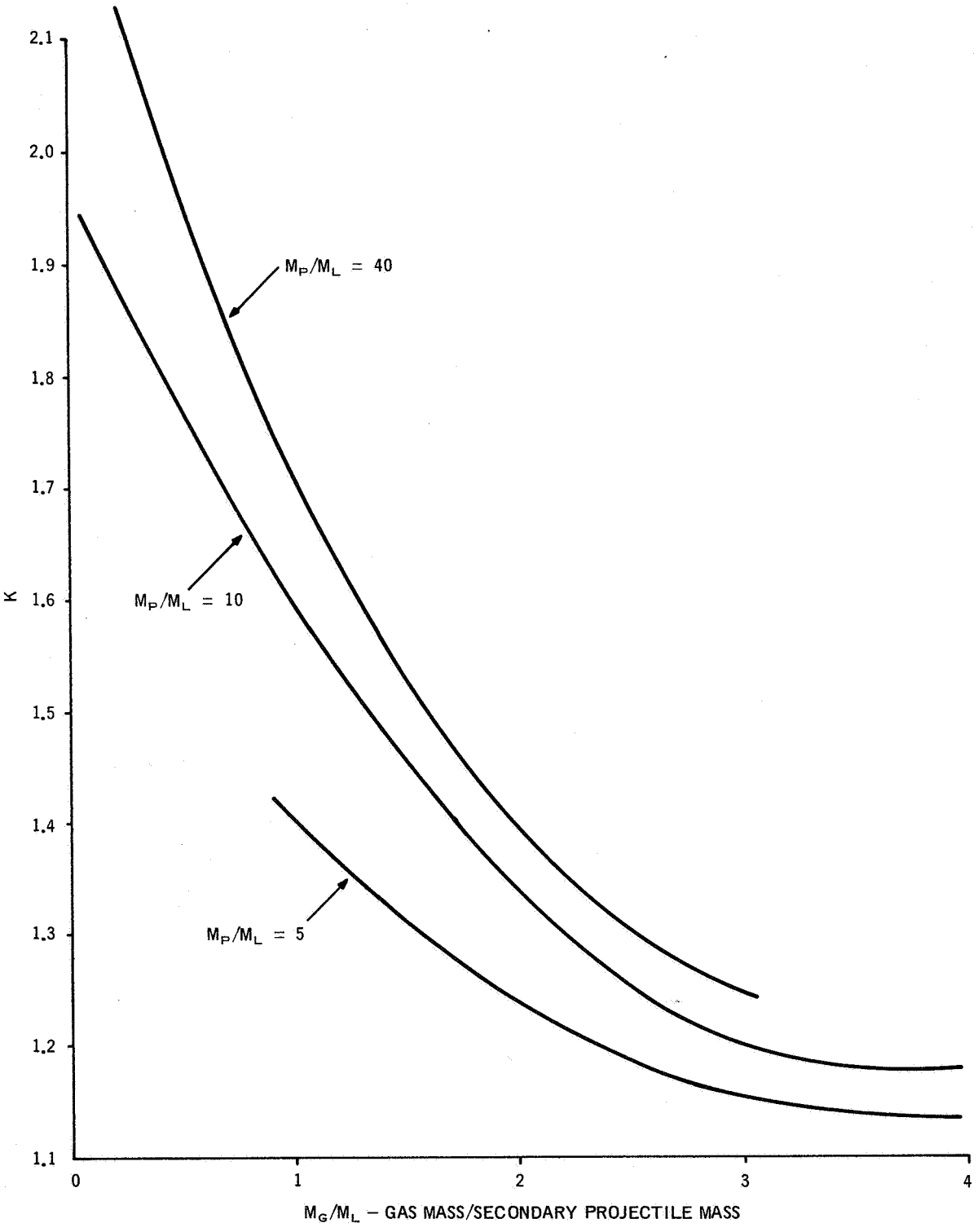

Figure 6. Variation of Energy Loss Factor 'K' with M_G/M_L - Criterion (b)

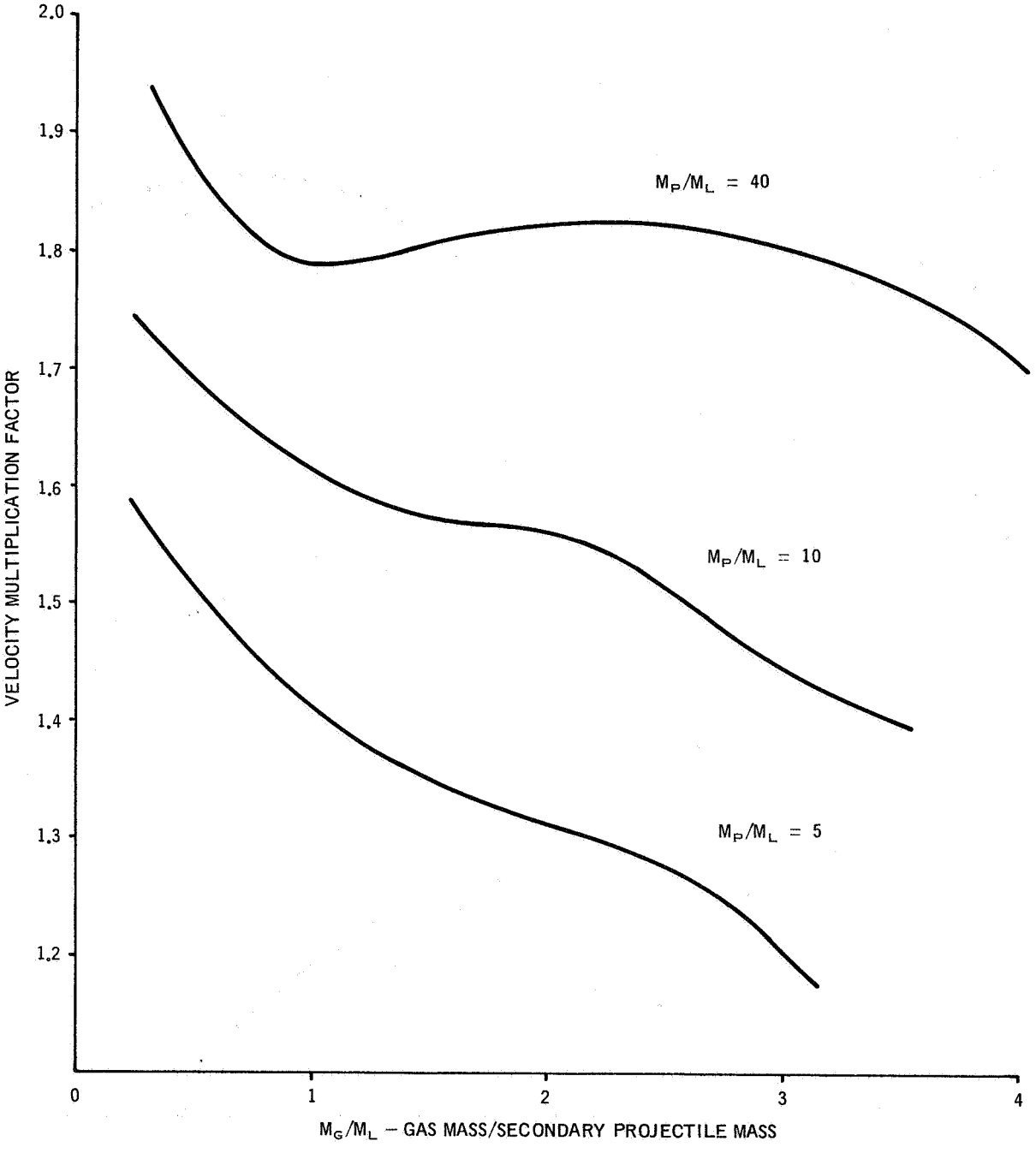

Figure 7. Velocity Multiplication Factors for Criterion (a)

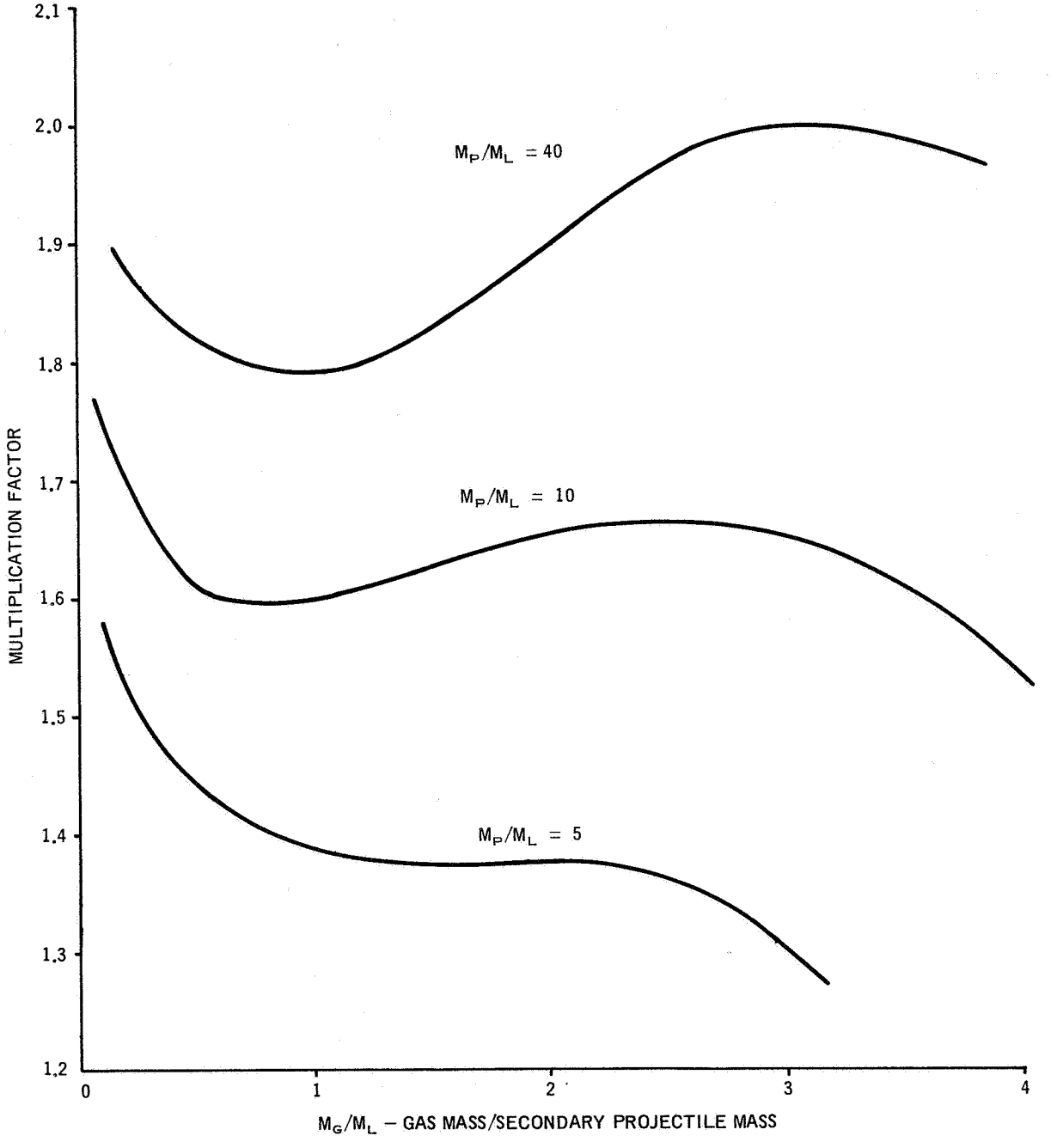

Figure 8. Velocity Multiplication Factors for Criterion (b)

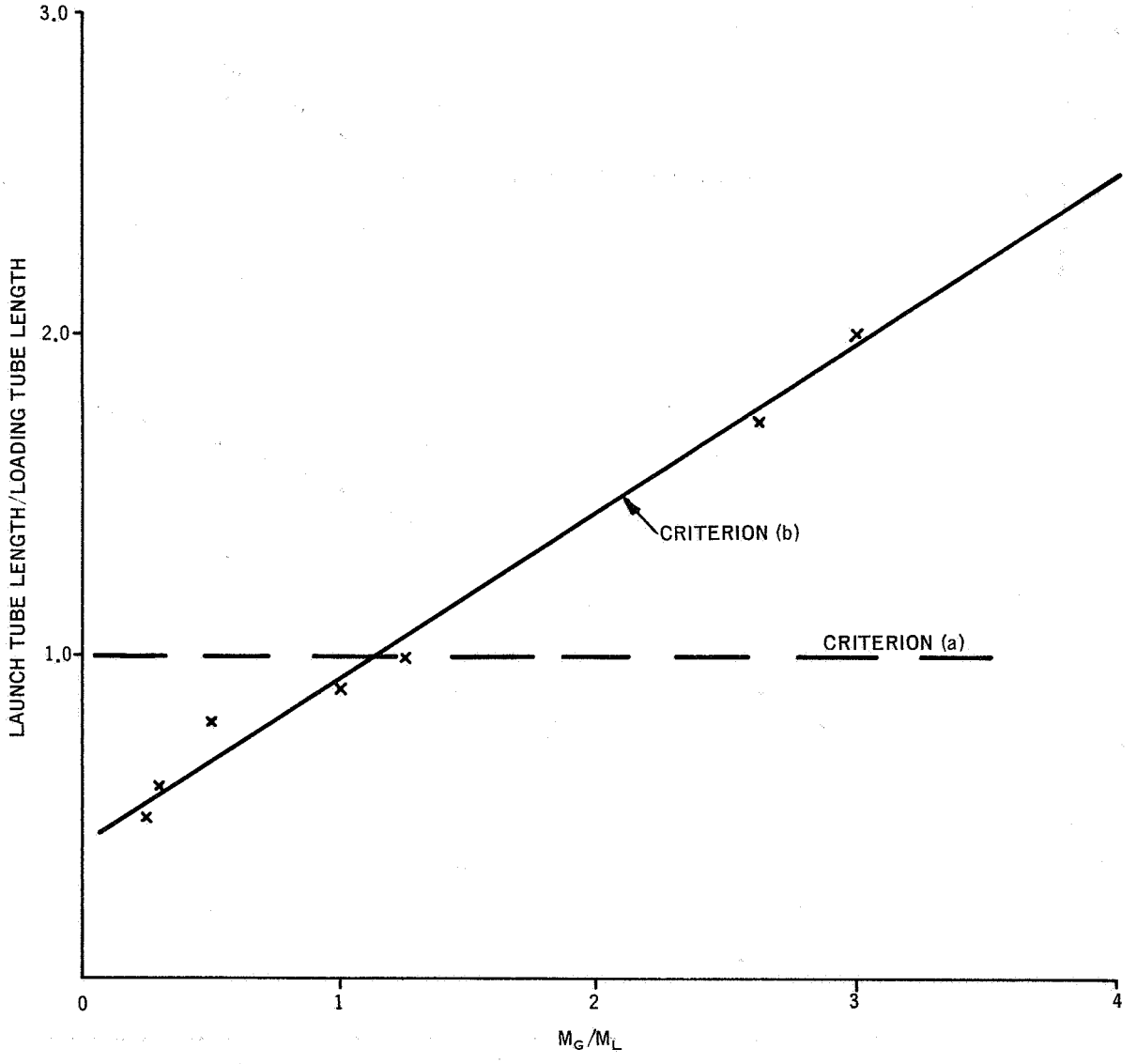

Figure 9. Launch Tube Length Required to Satisfy Criterion (b)

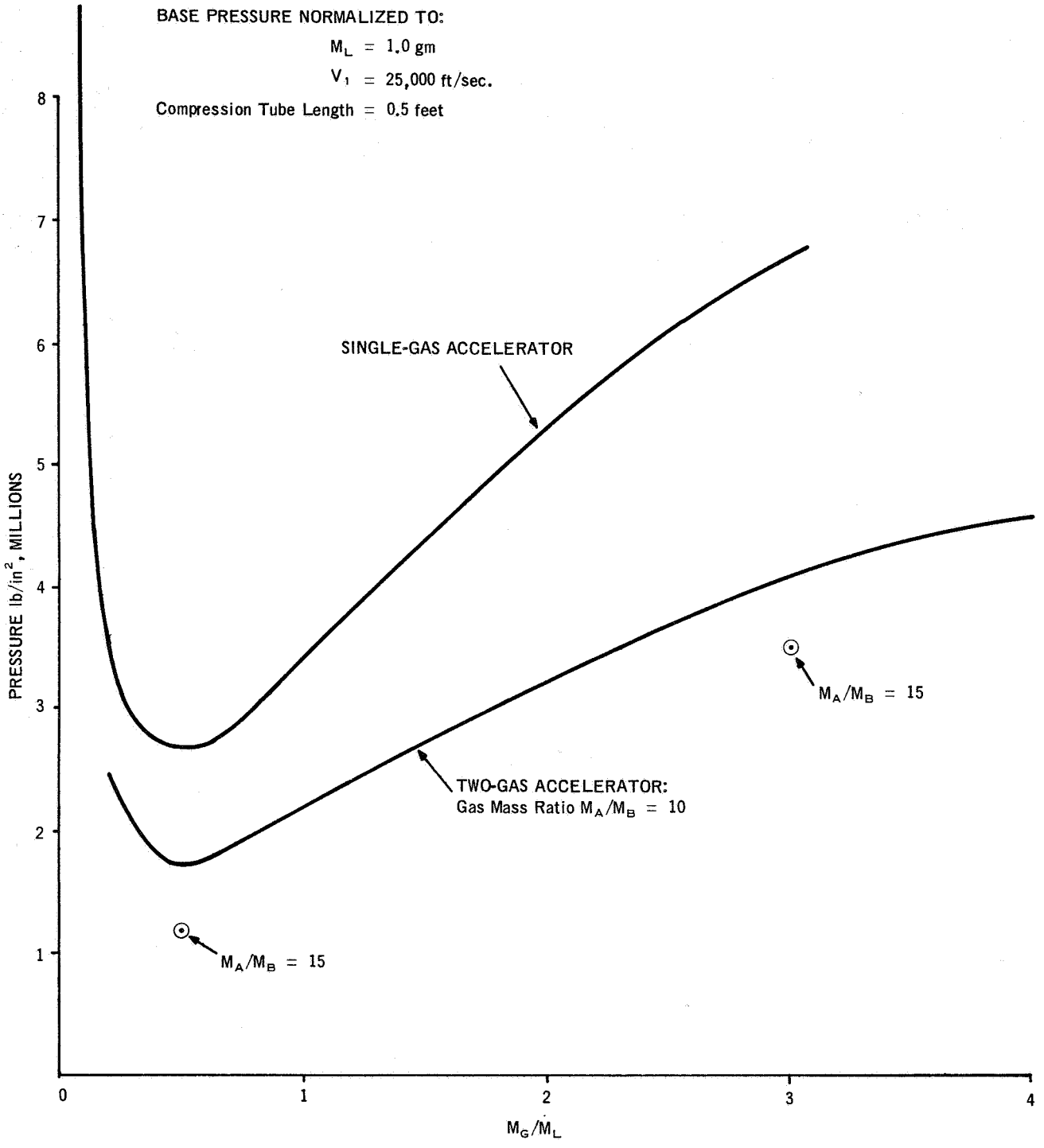

Figure 10. Normalized Base Pressure for Single-Gas and Two-Gas Accelerators

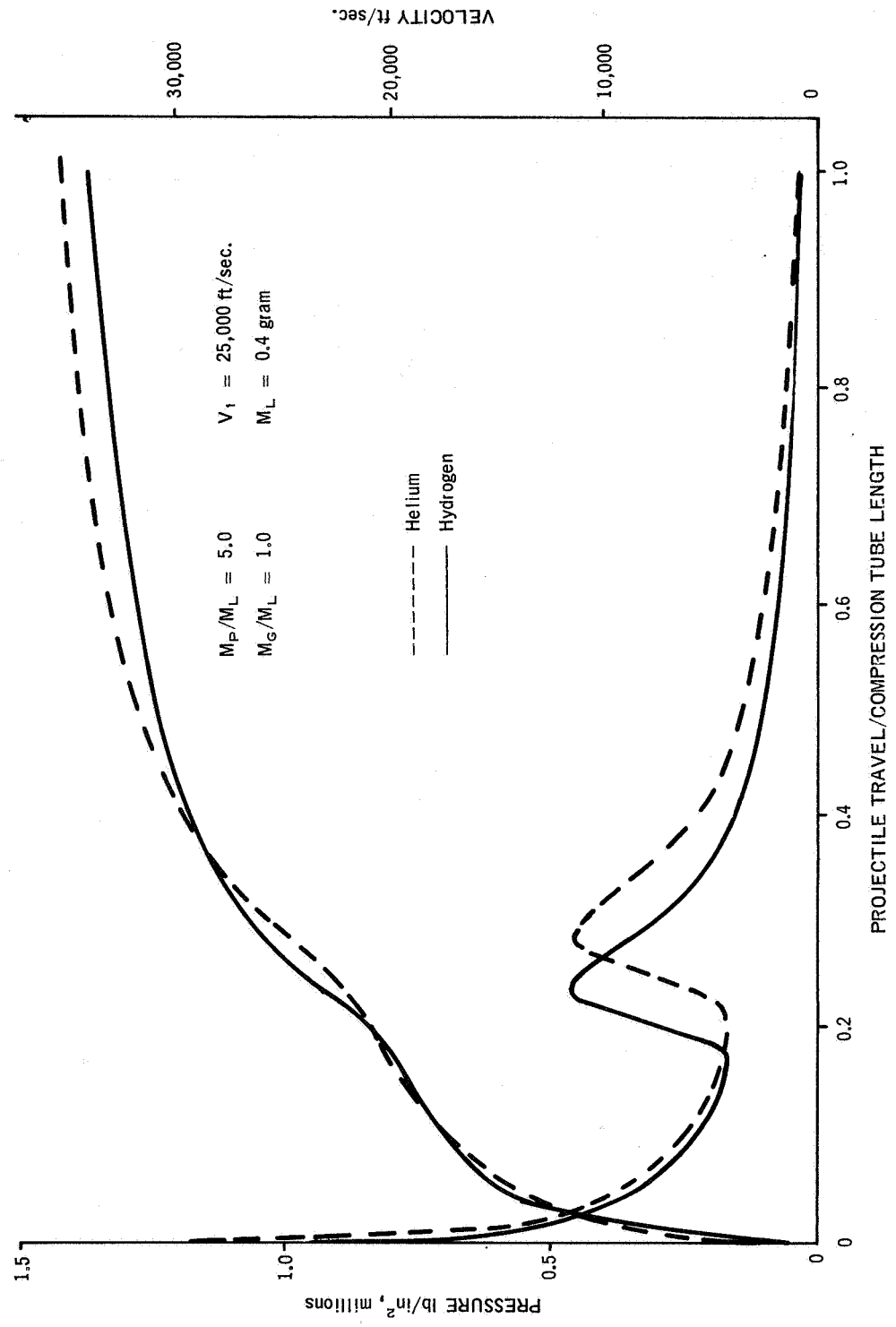

Figure 11. Typical Computed Base Pressure Histories for Helium and Hydrogen at $M_G/M_L = 1.0$

Figure 11.

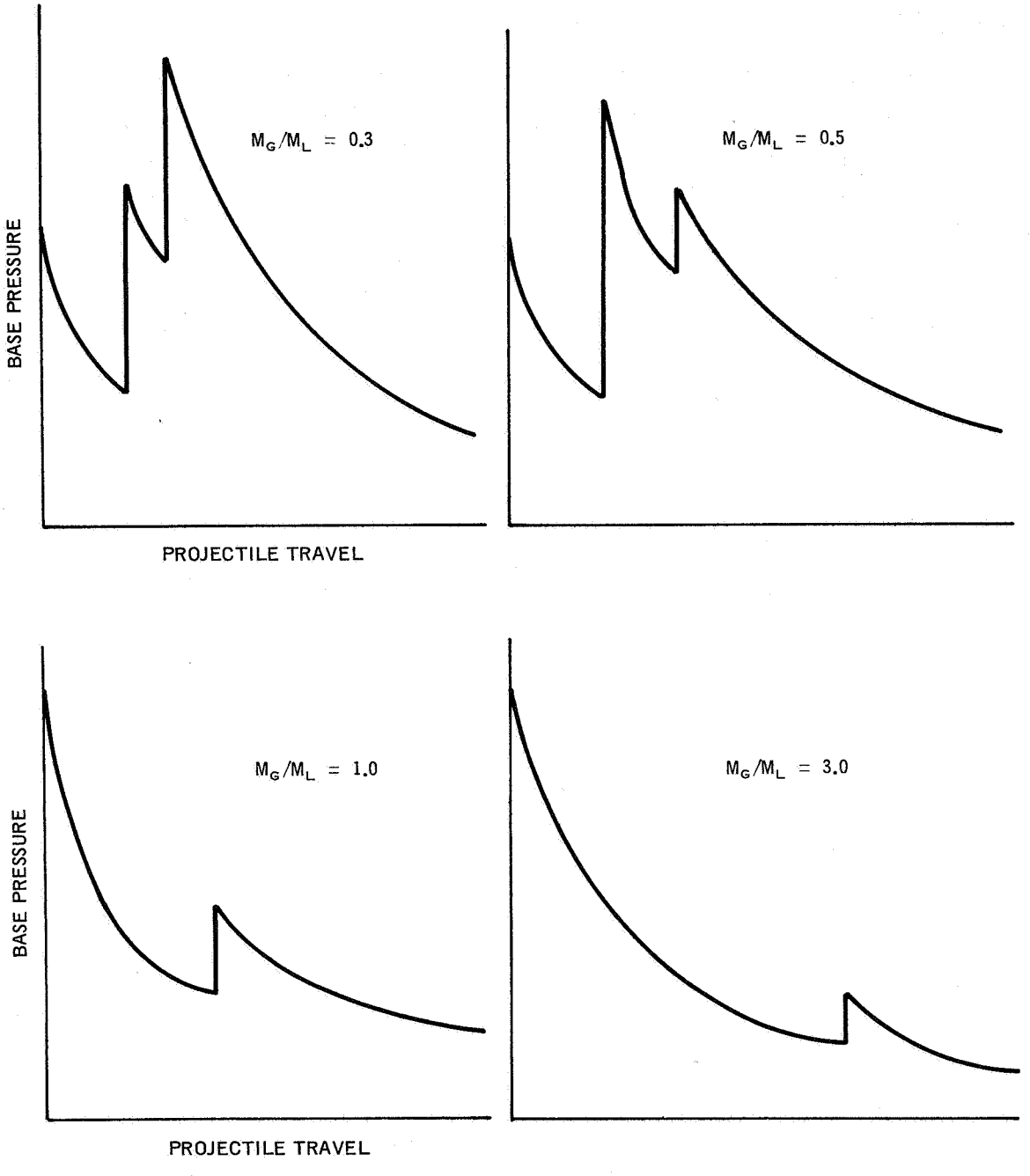

Figure 12. Base Pressure Histories in Single-Gas Accelerator

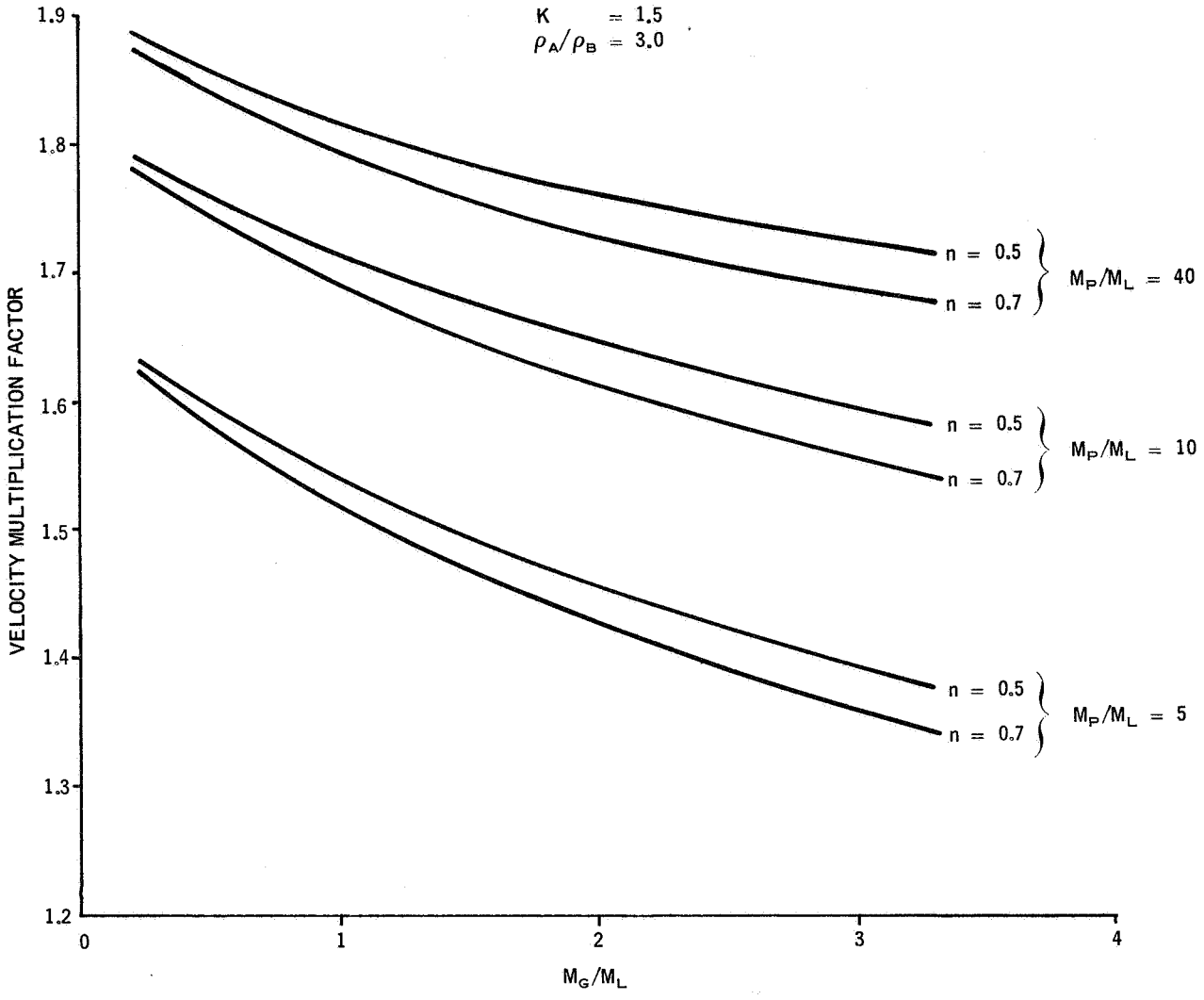

Figure 13. Typical Multiplication Factors from Simplified Analysis - Two-Gas Accelerator

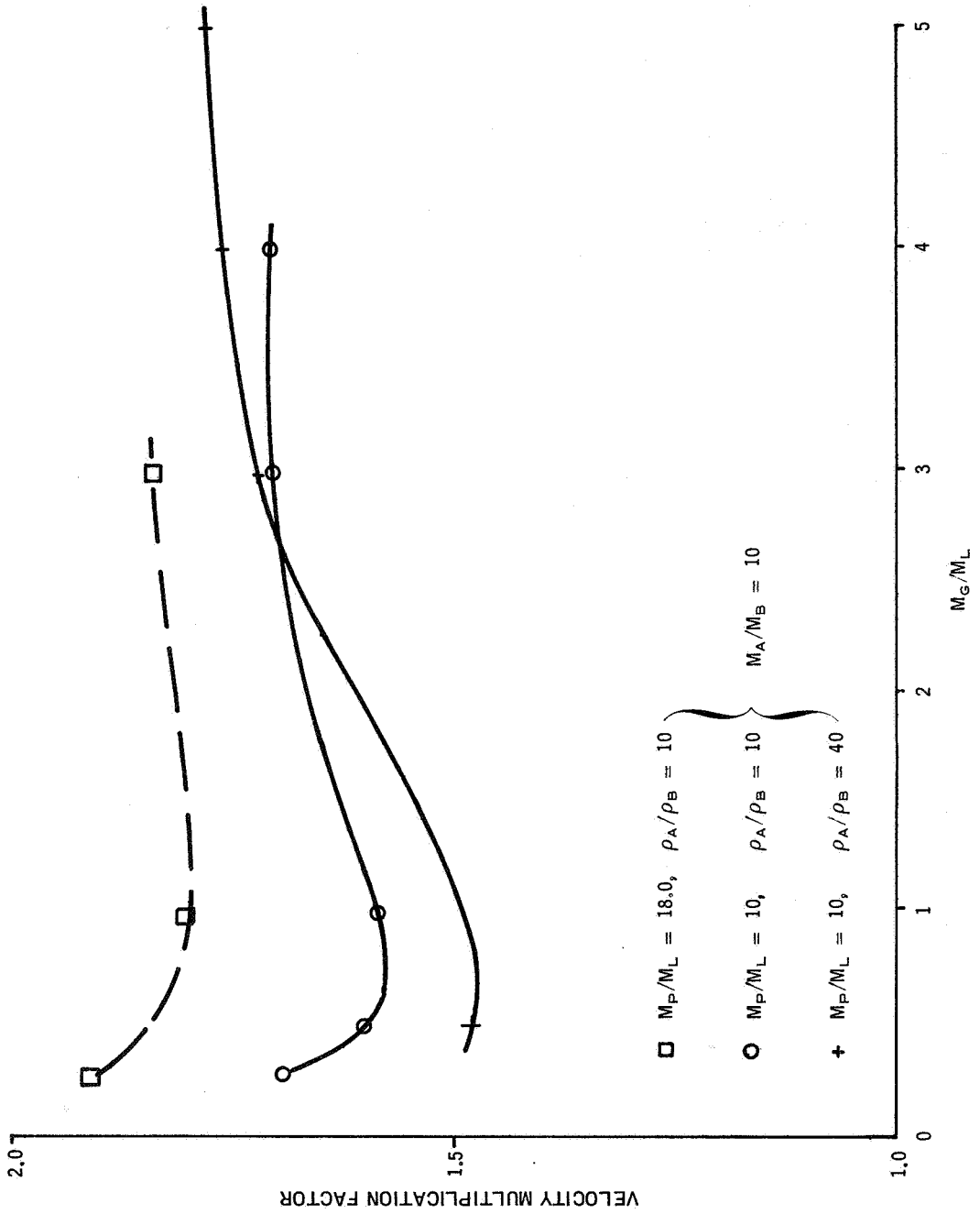

Figure 14. Velocity Multiplication for Two-Gas Accelerator (Computed)

Figure 14.

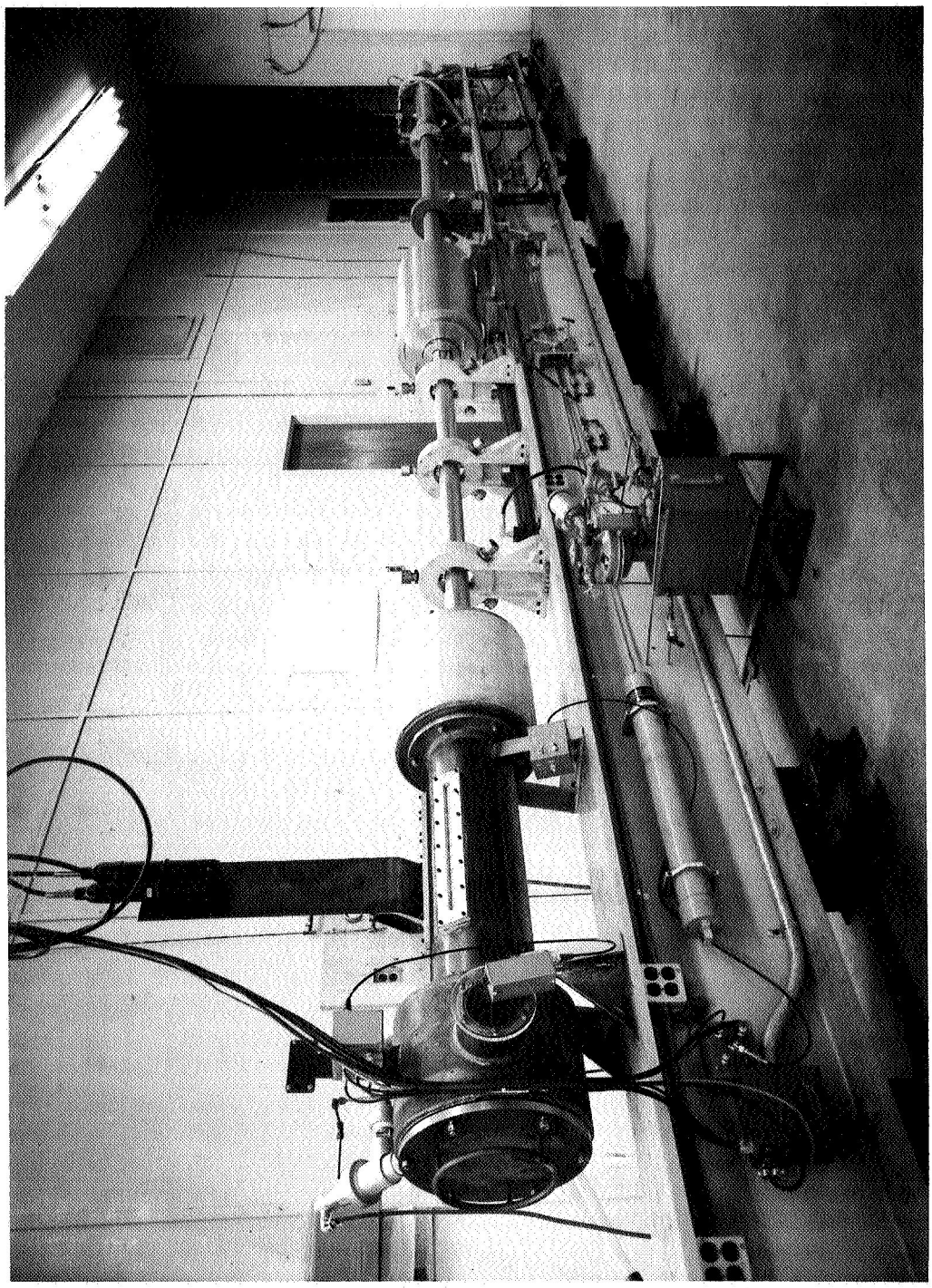

Figure 15. Light Gas Gun and Range Tank

Figure 15.

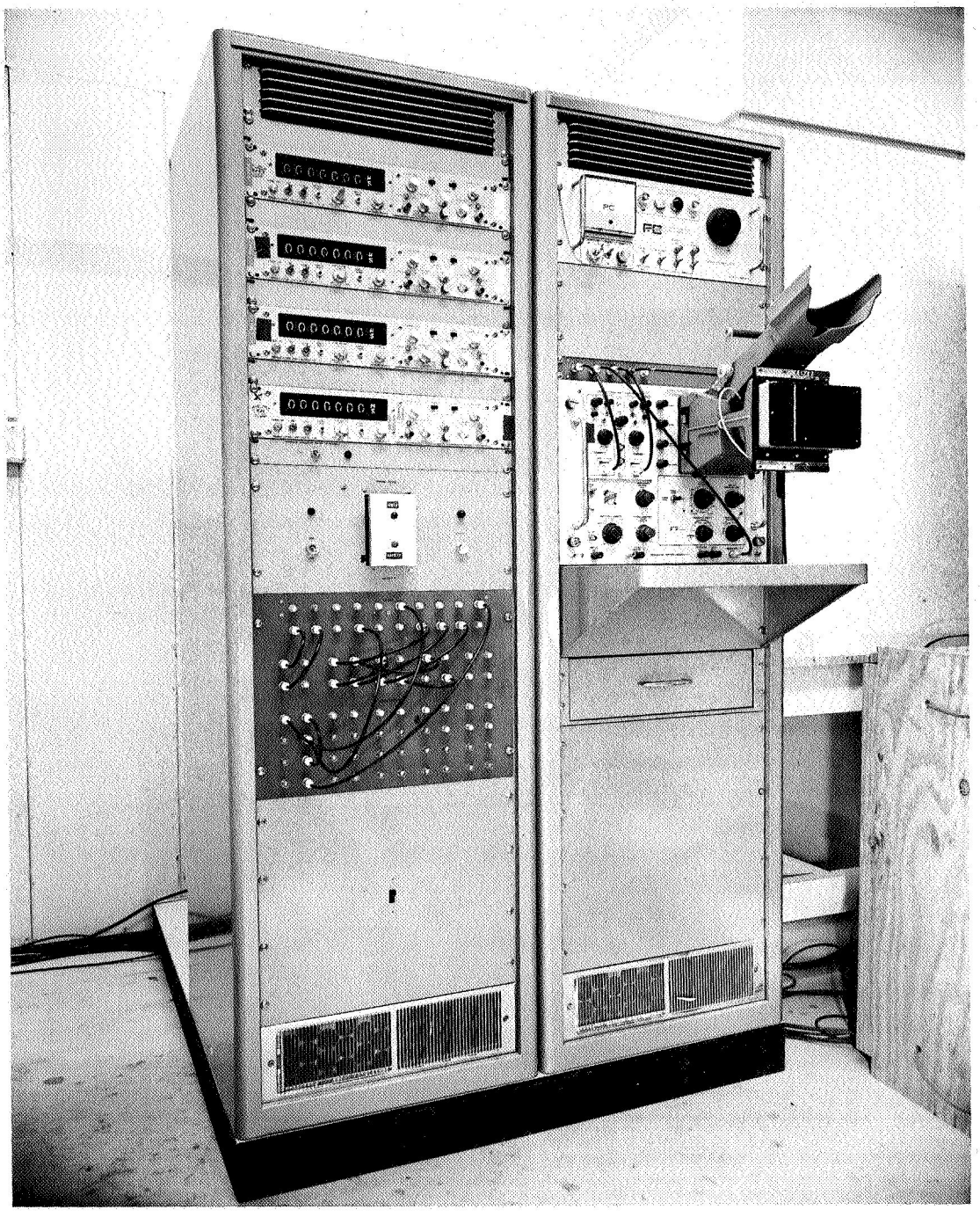

Figure 16. Instrumentation - Control Area

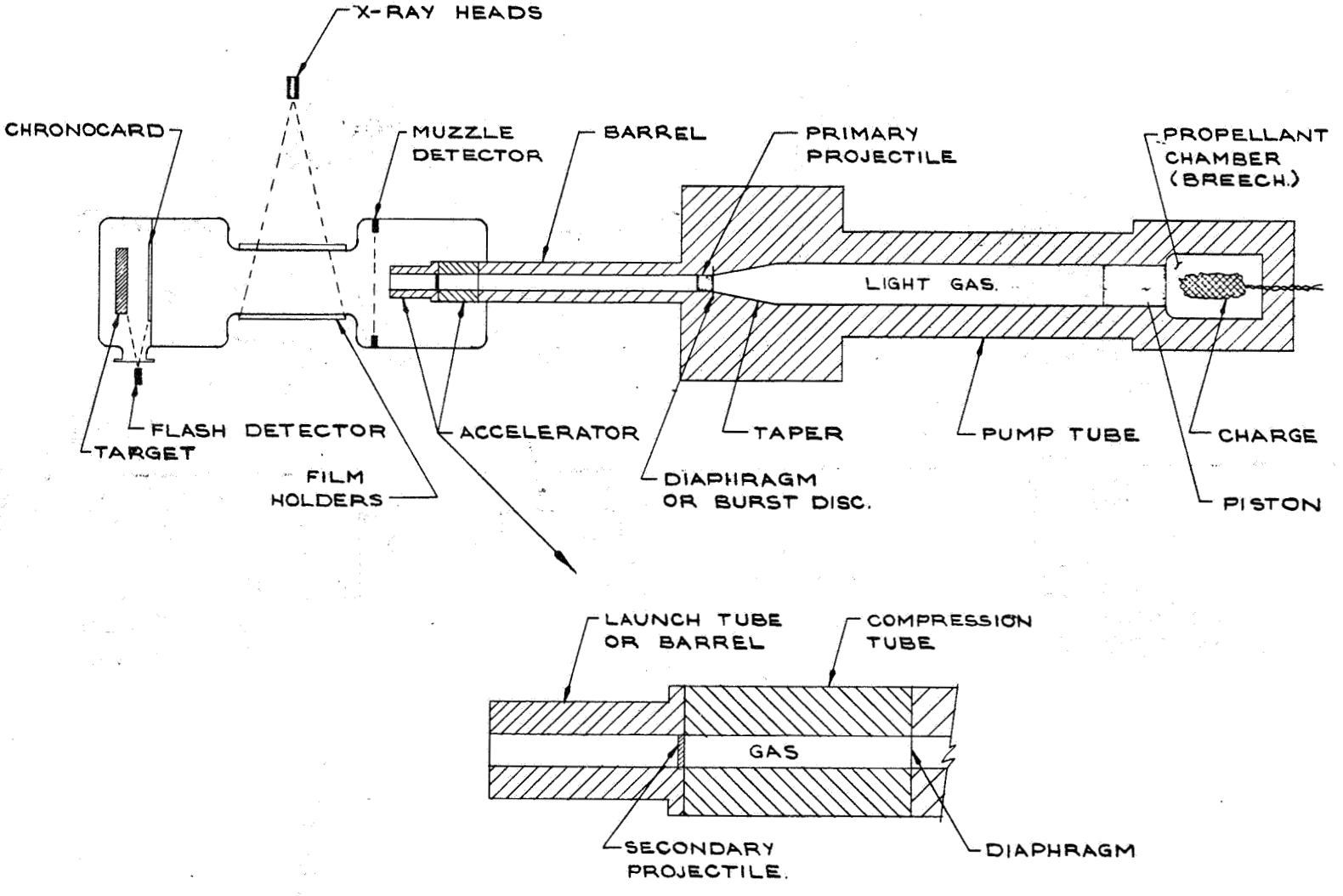

Figure 17. Light Gas Gun, Accelerator and Range Tank

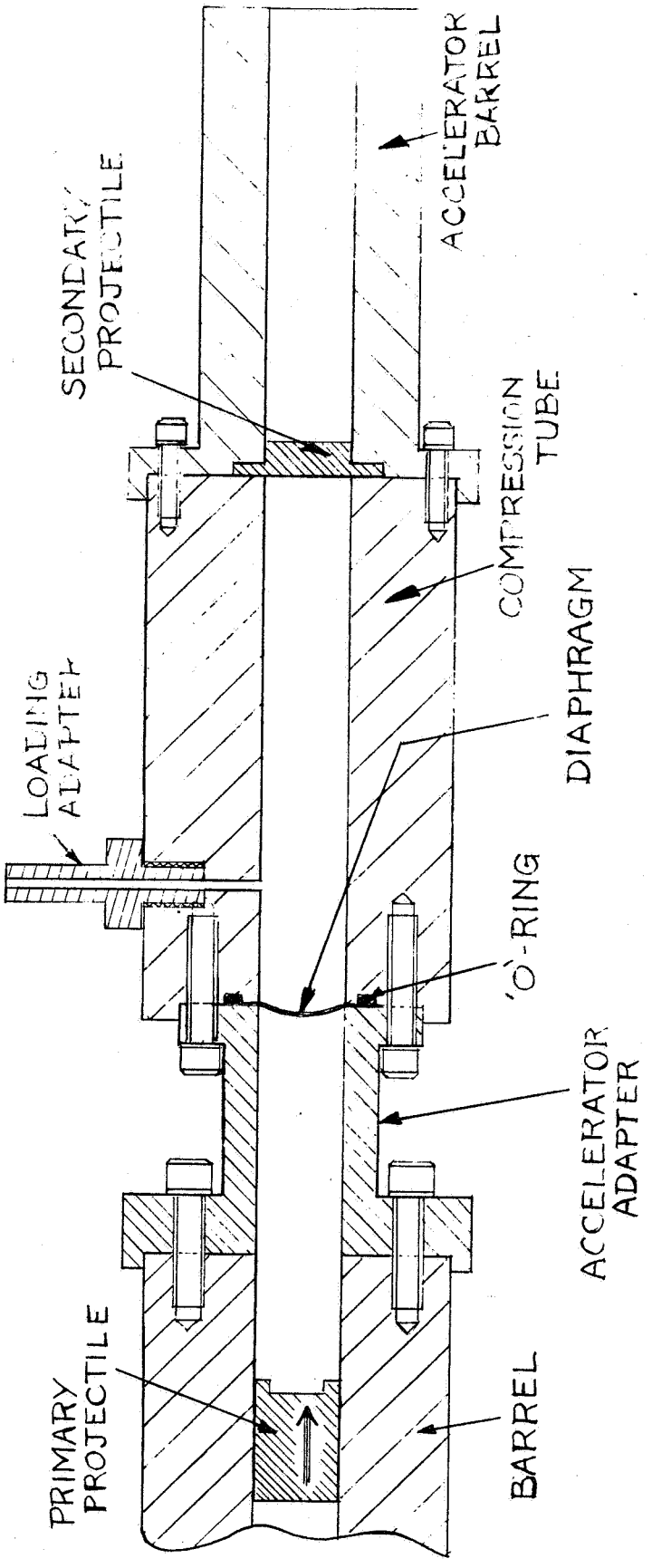

Figure 18. Constant Area Accelerator (Configuration 2)

Figure 18.

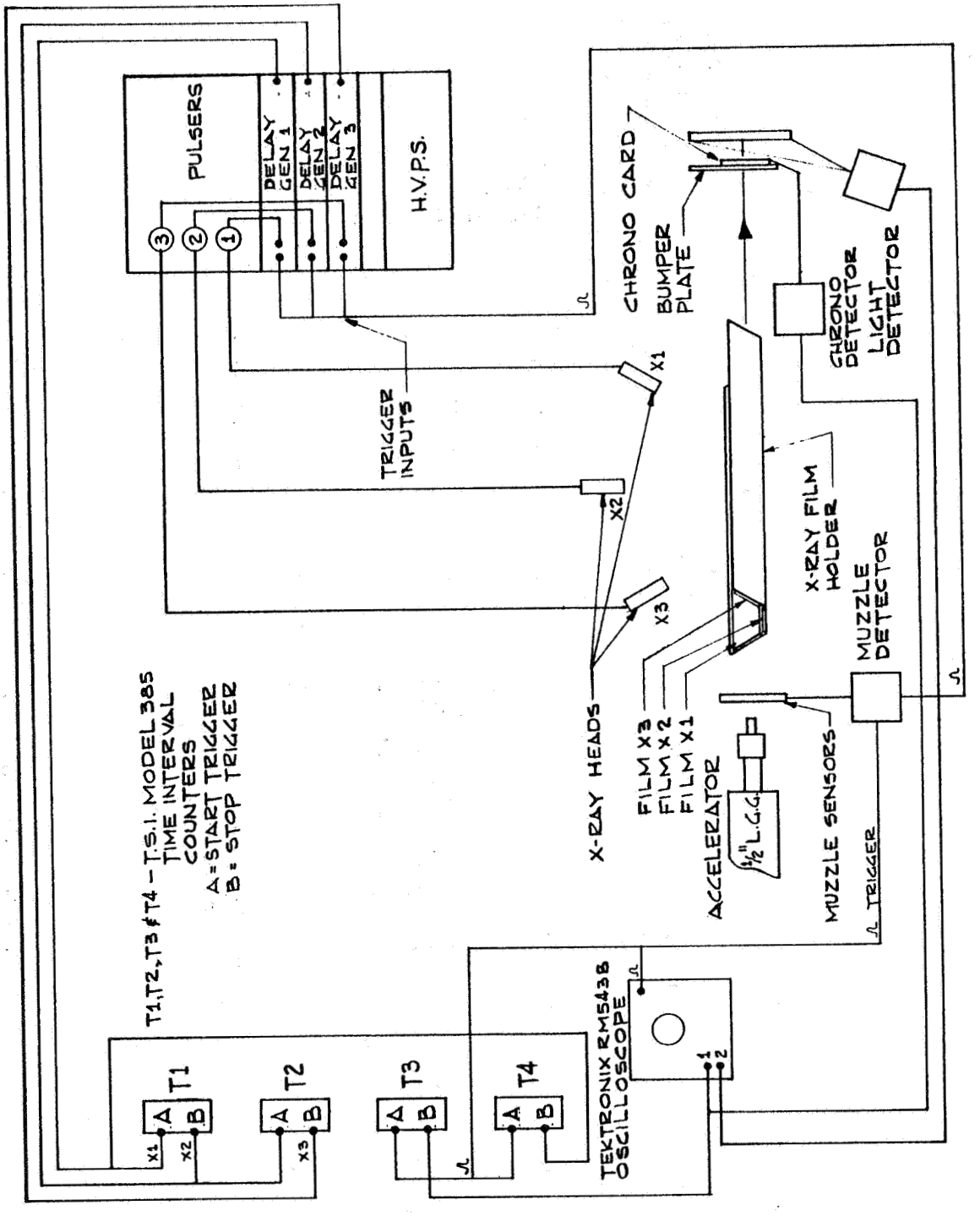

Figure 19. Instrumentation Equipment - Function Block Schematic Diagram

Figure 19.

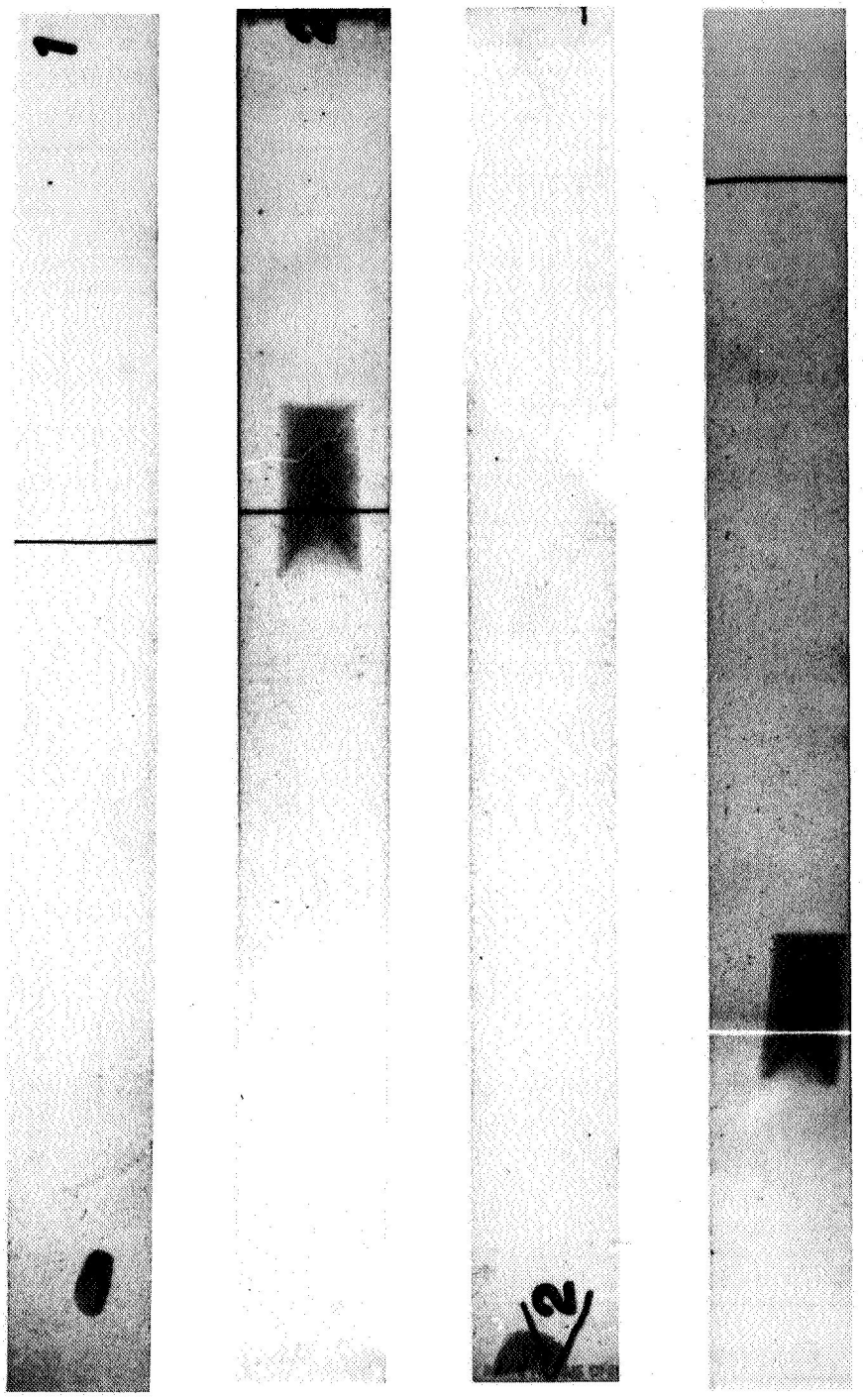

Figure 20. X-ray Photographs for Firing 634

Figure 20.

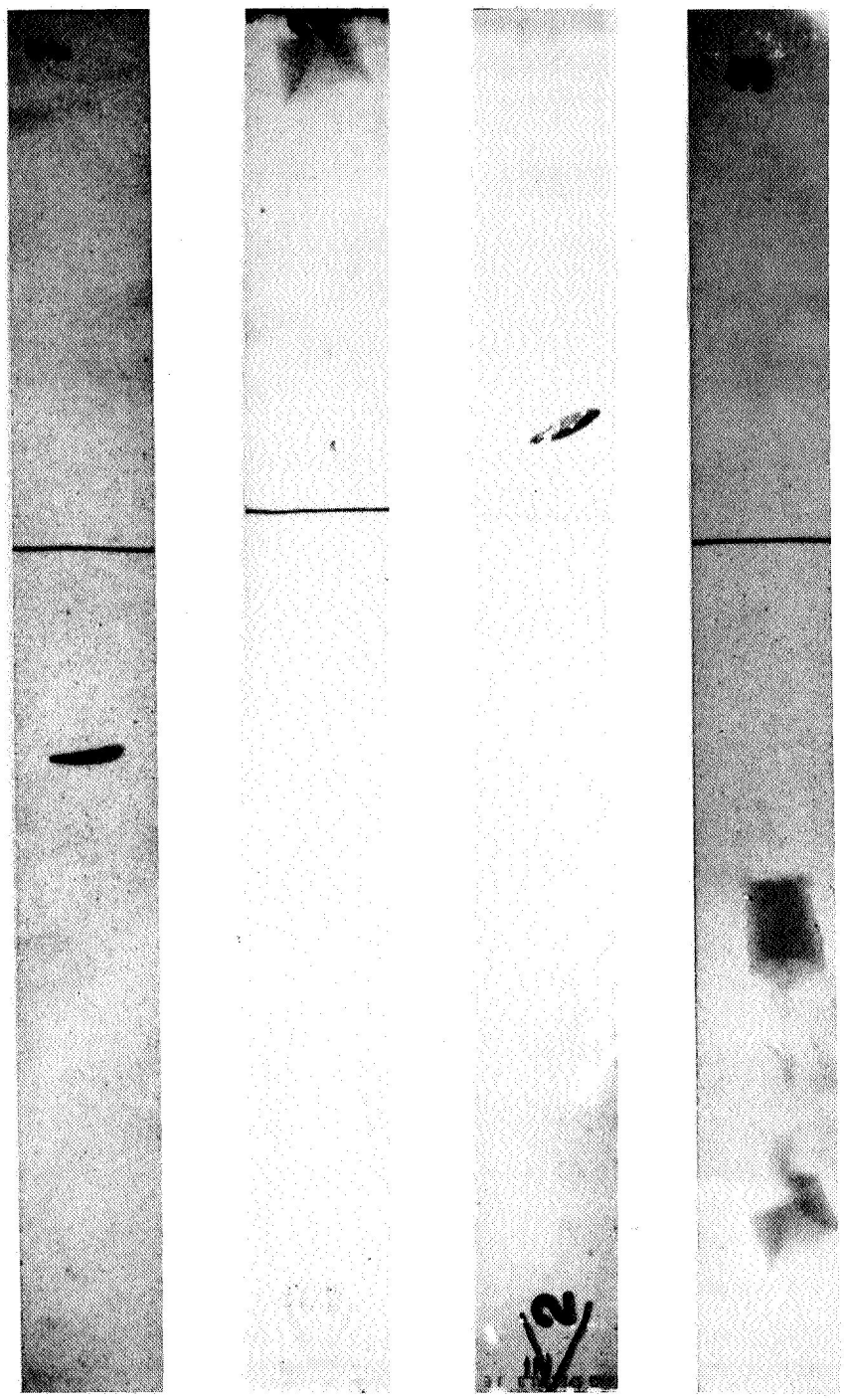

Figure 21. X-ray Photographs for Firing 635

Figure 21.

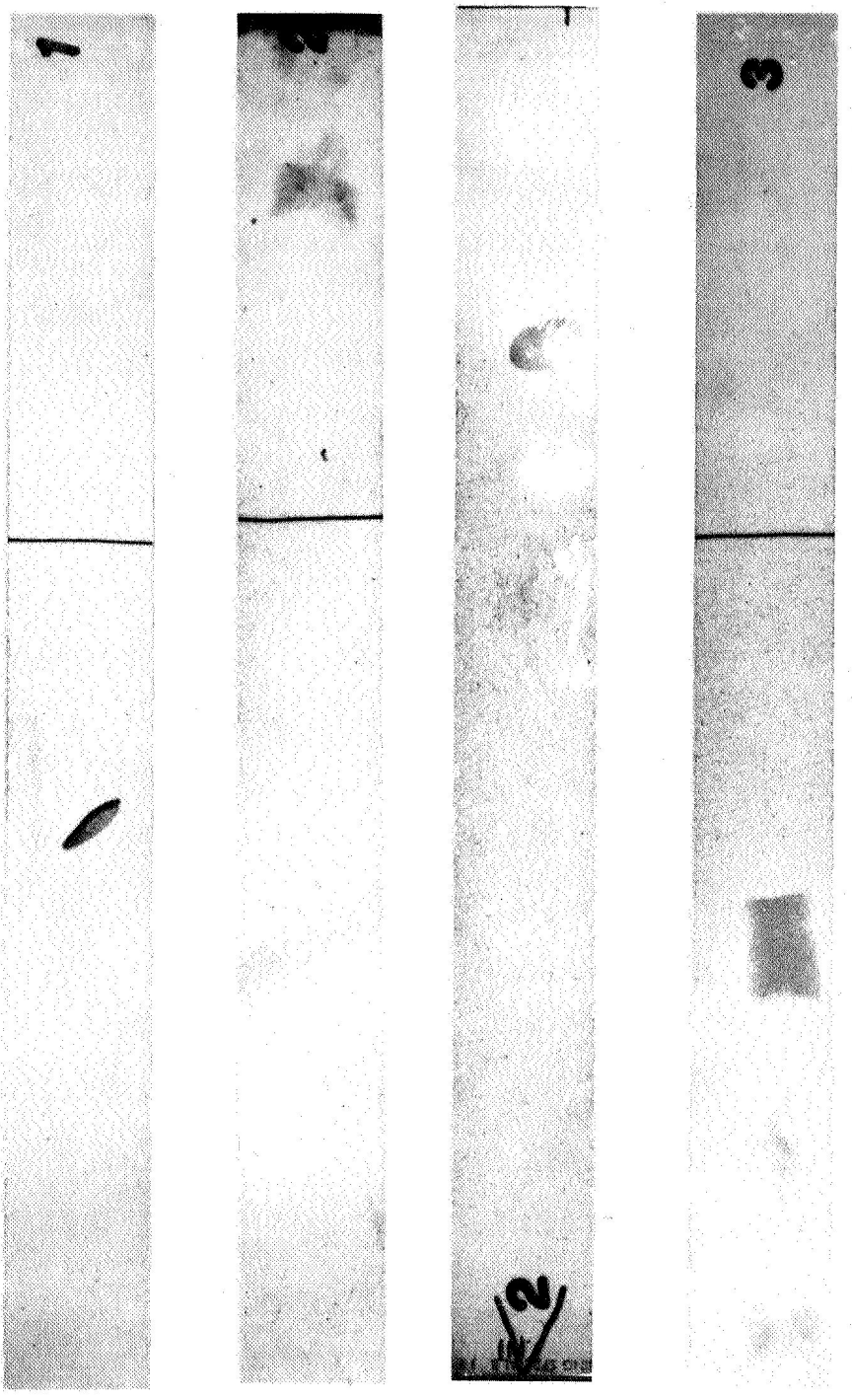

Figure 22. X-ray Photographs for Firing 636.

Figure 22.

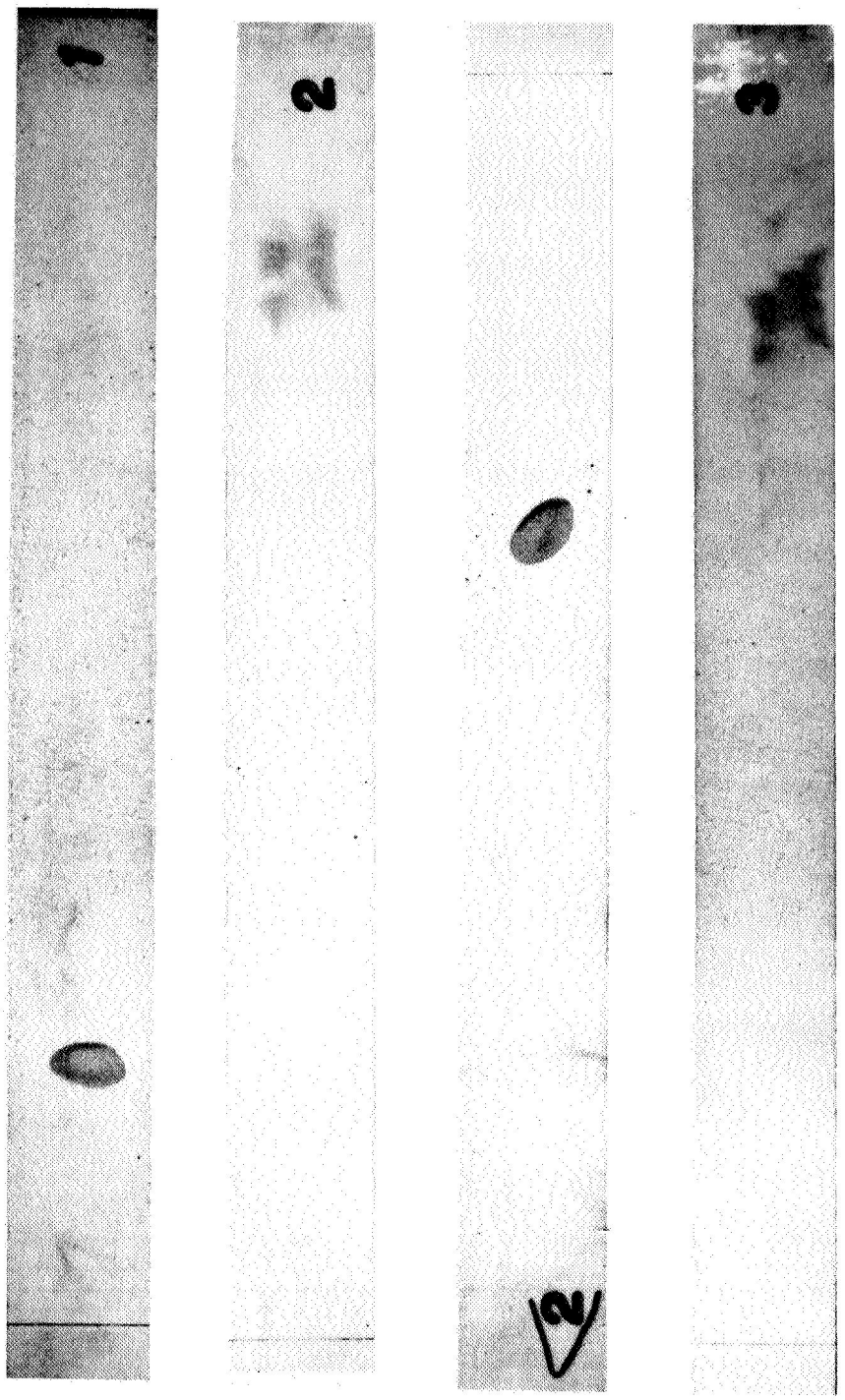

Figure 23. X-ray Photographs for Firing 637

Figure 23.

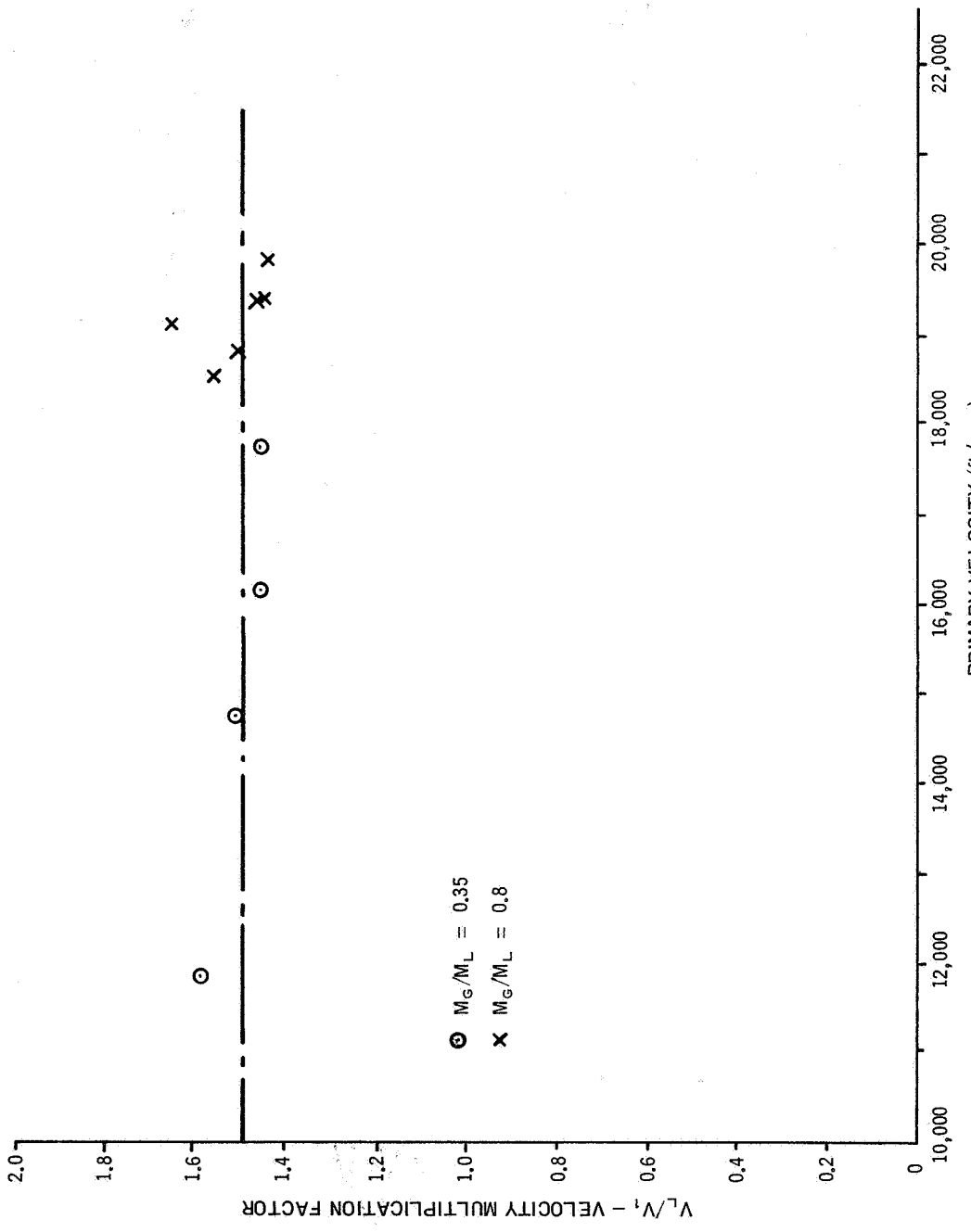

Figure 24. Experimental Velocity Multiplication Factor versus Primary Velocity

Figure 24.

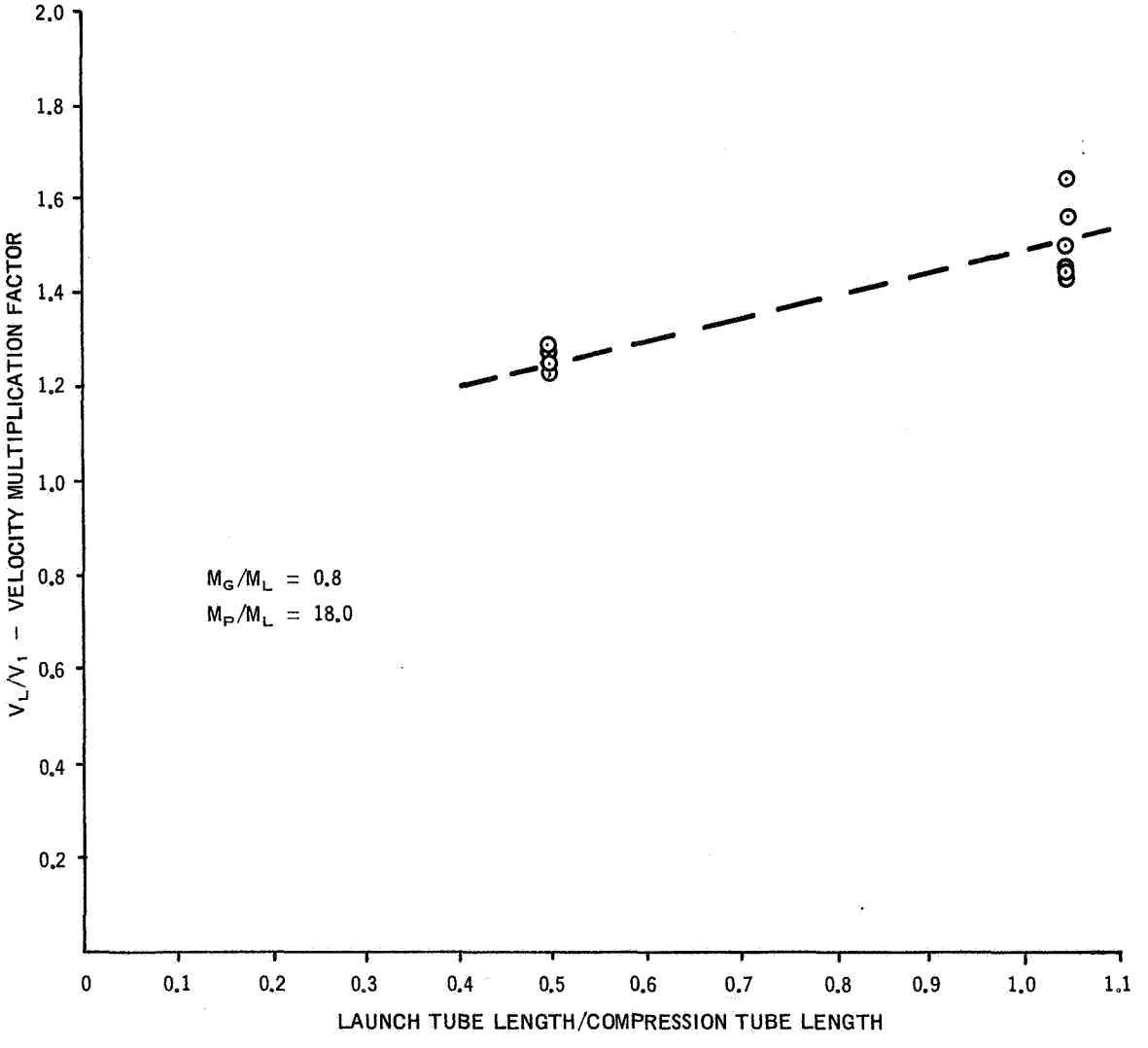

Figure 25. Experimental Velocity Multiplication Factor versus Launch Tube Length

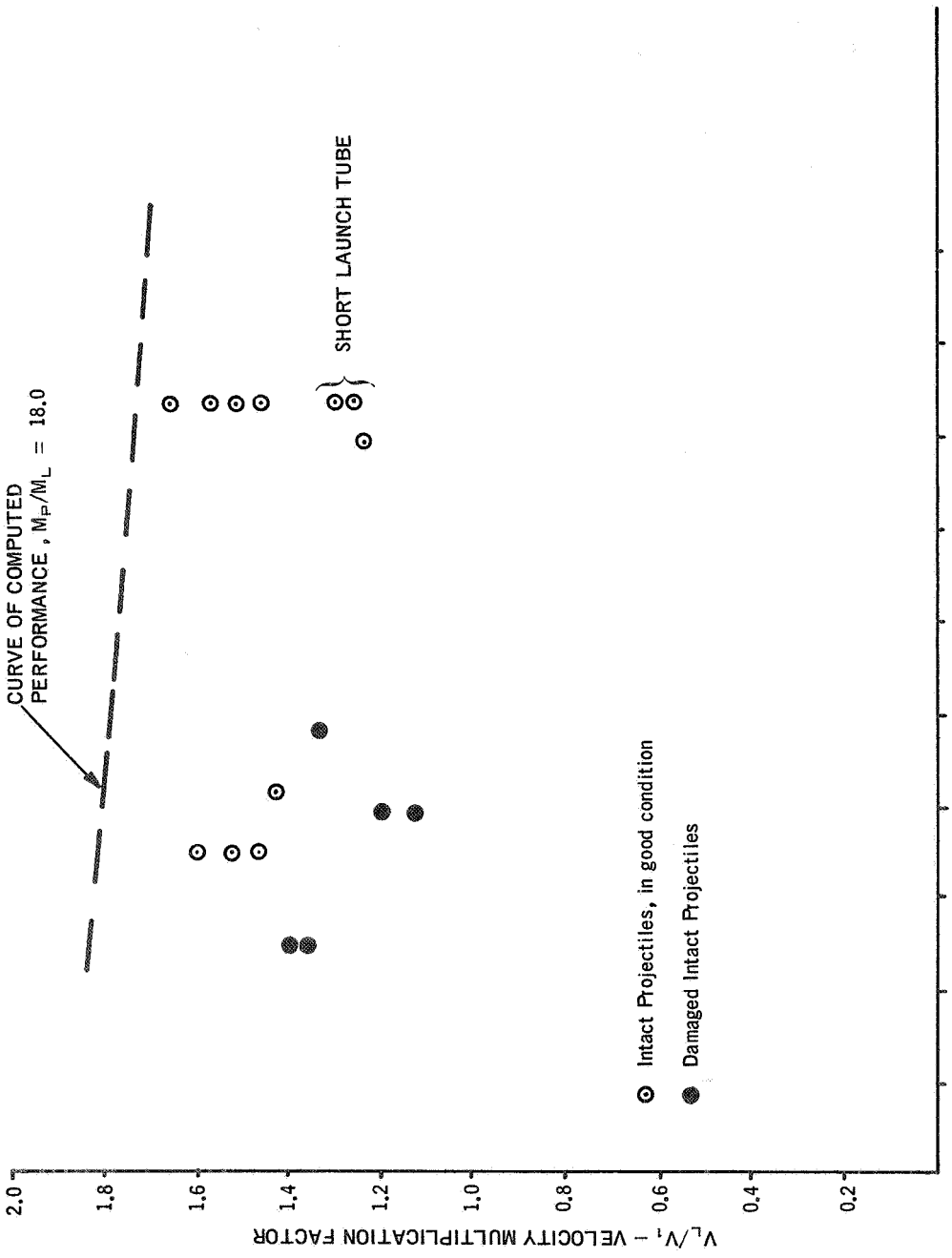

Figure 26. Experimental Velocity Multiplication Factor versus M_G/M_L

Figure 26.

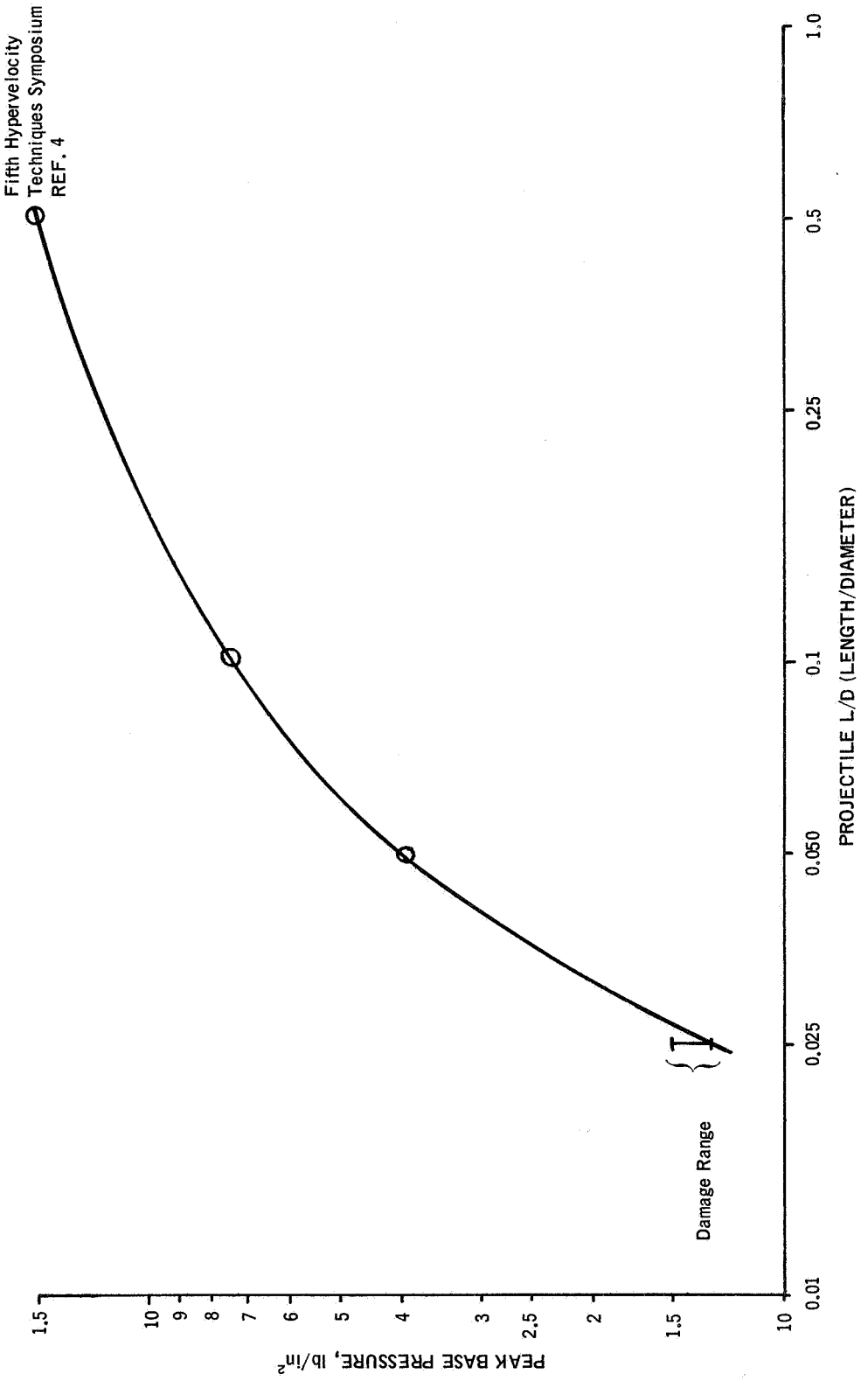

Figure 27. Observed Base Pressure Capability of Disk-Like Projectiles

Figure 27.

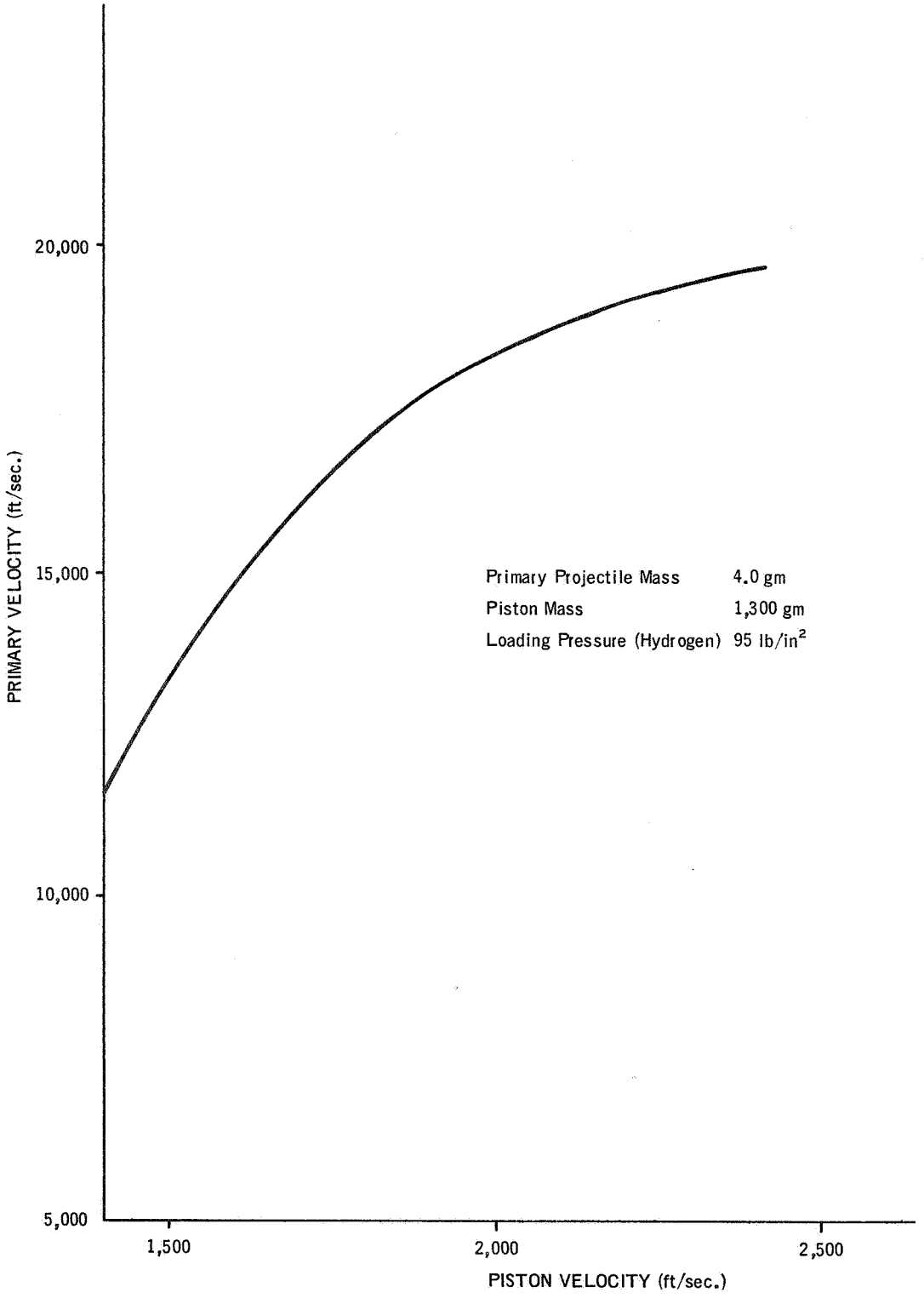

Figure 28. Light Gas Gun Primary Velocity versus Piston Velocity

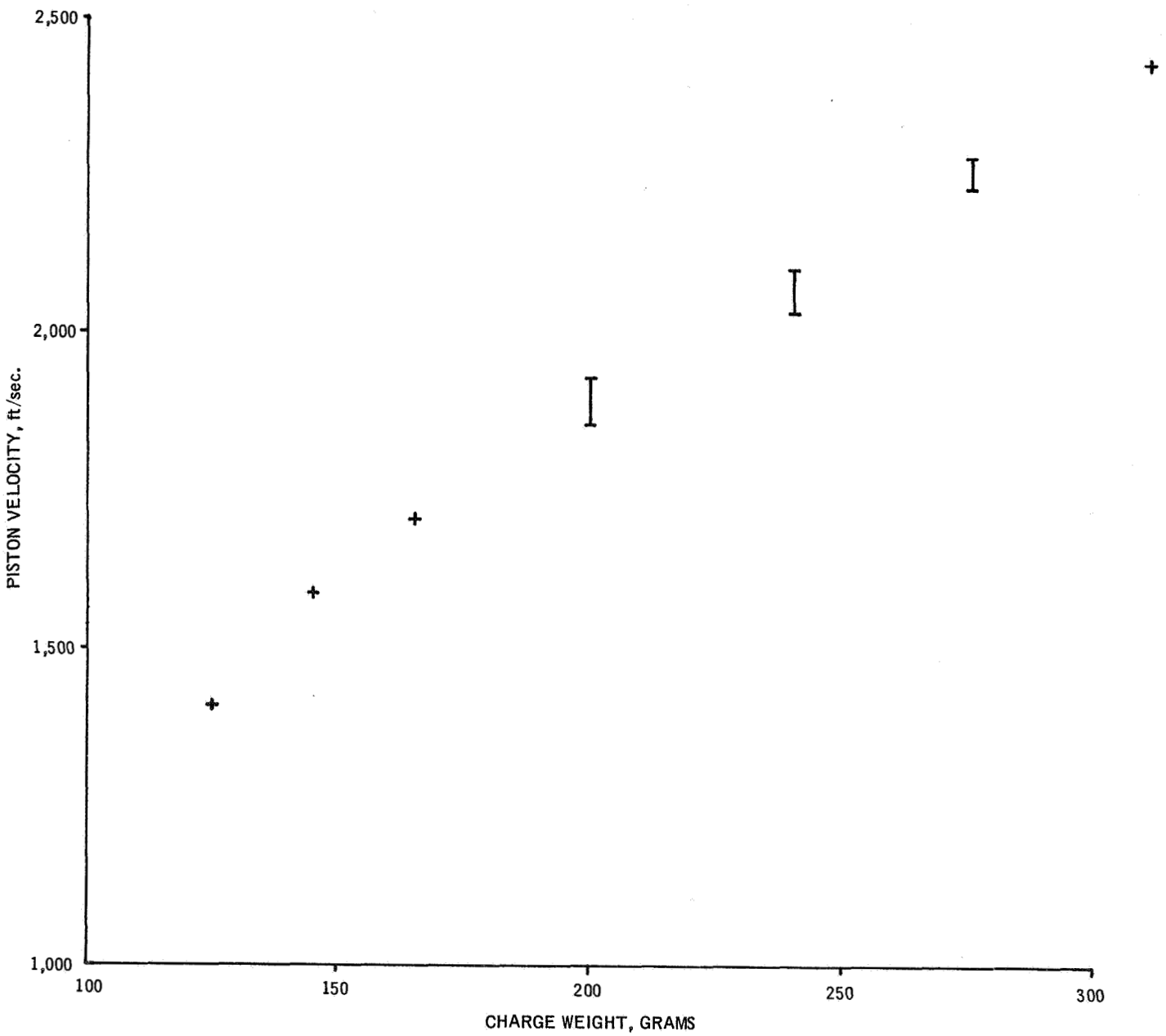

Figure 29. Piston Velocity versus Charge Weight, Hivel No. 2 Propellant

Printed and published in Canada by
Computing Devices
OF CANADA LIMITED